AD-A262 729

DTIC
ELECTE
APR 1 3 1993
S C D

(2)

ARMY RESEARCH LABORATORY

Pressure Oscillations in a Regenerative Liquid Propellant Gun and Influence of Random Processes

Gloria P. Wren
U.S. ARMY RESEARCH LABORATORY

Paul S. Gough
PAUL GOUGH ASSOCIATES, INC.

ARL-TR-103

March 1993

93 4 12 068

93-07634

50p

APPROVED FOR PUBLIC RELEASE; DISTRIBUTION IS UNLIMITED

NOTICES

Destroy this report when it is no longer needed. DO NOT return it to the originator.

Additional copies of this report may be obtained from the National Technical Information Service, U.S. Department of Commerce, 5285 Port Royal Road, Springfield, VA 22161.

The findings of this report are not to be construed as an official Department of the Army position, unless so designated by other authorized documents.

The use of trade names or manufacturers' names in this report does not constitute indorsement of any commercial product.

REPORT DOCUMENTATION PAGE

Form Approved
OMB No. 0704-0188

Public reporting burden for this collection of information is estimated to average 1 hour per response, including the time for reviewing instructions, searching existing data sources, gathering and maintaining the data needed, and completing and reviewing the collection of information. Send comments regarding this burden estimate or any other aspect of this collection of information, including suggestions for reducing this burden to Washington Headquarters Services, Directorate for Information Operations and Reports, 1215 Jefferson Davis Highway, Suite 1204, Arlington, VA 22202-4302 and to the Office of Management and Budget, Paperwork Reduction Project (0704-0188), Washington, DC 20503

1. AGENCY USE ONLY *(Leave blank)*	2. REPORT DATE	3. REPORT TYPE AND DATES COVERED
	March 1993	Final, September 1990 - June 1991

4. TITLE AND SUBTITLE

Pressure Oscillations in a Regenerative Liquid Propellant Gun and Influence of Random Processes

5. FUNDING NUMBERS

PR: 1L162618AH80
DA 30 6709

6. AUTHOR(S)

Gloria P. Wren and Paul S. Gough*

7. PERFORMING ORGANIZATION NAME(S) AND ADDRESS(ES)

U.S. Army Research Laboratory
ATTN: AMSRL-WT-PA
Aberdeen Proving Ground, MD 21005-5066

8. PERFORMING ORGANIZATION REPORT NUMBER

9. SPONSORING/MONITORING AGENCY NAME(S) AND ADDRESS(ES)

U.S. Army Research Laboratory
AMSRL-OP-CI-B (Tech Lib)
Aberdeen Proving Ground, MD 21005-5066

10. SPONSORING/MONITORING AGENCY REPORT NUMBER

ARL-TR-103

11. SUPPLEMENTARY NOTES

* Paul Gough Associates, Portsmouth, NH

12a. DISTRIBUTION/AVAILABILITY STATEMENT

Approved for public release; distribution is unlimited.

12b. DISTRIBUTION CODE

13. ABSTRACT *(Maximum 200 words)*

A one-dimensional model of the regenerative liquid propellant gun (RLPG) interior ballistic cycle has been developed in which the jet breakup and energy release is governed by a Taylor formulation. The model allows a random component in the jet breakup to simulate conditions which may exist in the gun. The random component produces rough combustion with energy being released in a nonuniform manner. The resulting chamber pressure history exhibits oscillations qualitatively similar to those observed experimentally. Moreover, it is shown that even though the energy release is confined to the chamber, the oscillations can be propagated downbore to the base of the projectile, thereby presenting a potential hazard for sensitive munitions. A possible remedy is discussed.

14. SUBJECT TERMS

liquid propellants; combustion instability; oscillation; regenerative; pressure oscillations

15. NUMBER OF PAGES 45

16. PRICE CODE

17. SECURITY CLASSIFICATION OF REPORT	18. SECURITY CLASSIFICATION OF THIS PAGE	19. SECURITY CLASSIFICATION OF ABSTRACT	20. LIMITATION OF ABSTRACT
UNCLASSIFIED	UNCLASSIFIED	UNCLASSIFIED	UL

INTENTIONALLY LEFT BLANK.

TABLE OF CONTENTS

DTIC QUALITY INSPECTED 4

Accesion For	
NTIS CRA&I	☑
DTIC TAB	☐
Unannounced	☐
Justification	
By	
Distribution /	
Availability Codes	
Dist	Avail and / or Special
A-1	

INTENTIONALLY LEFT BLANK.

LIST OF FIGURES

INTENTIONALLY LEFT BLANK.

ACKNOWLEDGMENT

The authors acknowledge the invaluable assistance of Ms. Sharon Richardson of the U.S. Army Research Laboratory* (ARL), Aberdeen Proving Ground, MD, who performed many of the code runs and data presentations. In addition, the authors would like to thank the reviewers of this manuscript, Mr. Fred Robbins and Mr. William Oberle of ARL, for their comments.

* The U.S. Army Ballistic Research Laboratory (BRL) was deactivated on 30 September 1992 and subsequently became a part of ARL on 1 October 1992.

INTENTIONALLY LEFT BLANK.

1. INTRODUCTION

Experimental pressure-time curves from regenerative liquid propellant gun (RLPG) firings characteristically show the presence of high amplitude, high frequency pressure fluctuations in the combustion chamber as demonstrated in Figure 1. The graph in Figure 1 is taken from a combustion chamber gage for a 155-mm RLPG firing. The gun was built under contract by the General Electric Company for the U.S. Army. Broadband high-frequency (0–75 kHz), high-amplitude (up to 30% of mean pressure) pressure oscillations have occurred in virtually all regenerative liquid propellant gun firings, including all calibers and diverse injection patterns studied nationally and internationally (Cook 1990; Klingenberg 1991; Haberl 1991; and Rychanovsky 1991). The origin of these pressure fluctuations, their propagation, and their influence on gun components are areas of active study in a number of programs sponsored by the U.S. Army. The oscillations may propagate downtube and cause the pressure at the base of the projectile to fluctuate as well, a potential source of concern for munitions compatibility (Bannister et al. 1991).

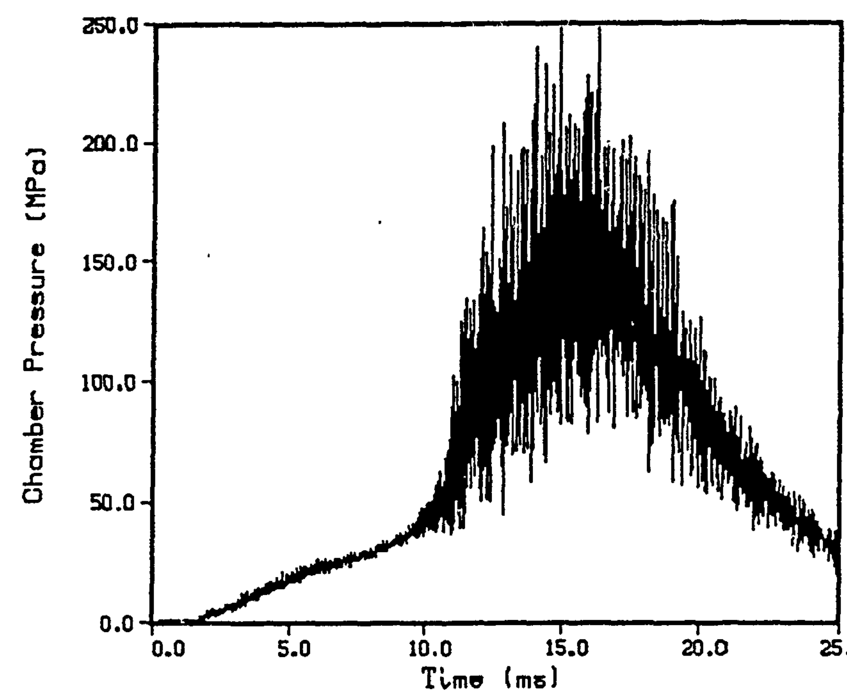

Figure 1. Experimental combustion chamber pressure history from a 155-mm regenerative liquid propellant gun.

A schematic of the RLPG developed in the United States is shown in Figure 2 and is referred to as a Concept VIC design. An external solid or liquid propellant igniter (not shown) venting into the combustion chamber initiates the ballistic cycle. The control (inner) piston moves first in response to the combustion chamber pressure rise, and its motion is modulated by the pressure in the damper. The injection (outer) piston follows the control piston in response to the chamber and liquid pressures acting on the exposed surface areas. The liquid propellant, LGP1846 (now called XM46), flows through the annulus created between the two moving pistons into the combustion chamber, where it burns, accelerating the projectile. Liquid propellant gun mean performance (data with oscillations removed by filtering) is modeled with a mature, predictive, lumped parameter, interior ballistic model which has been compared extensively to experimental data (Coffee, Wren, and Morrison 1989, 1990; Wren, Coffee and Morrison 1991).

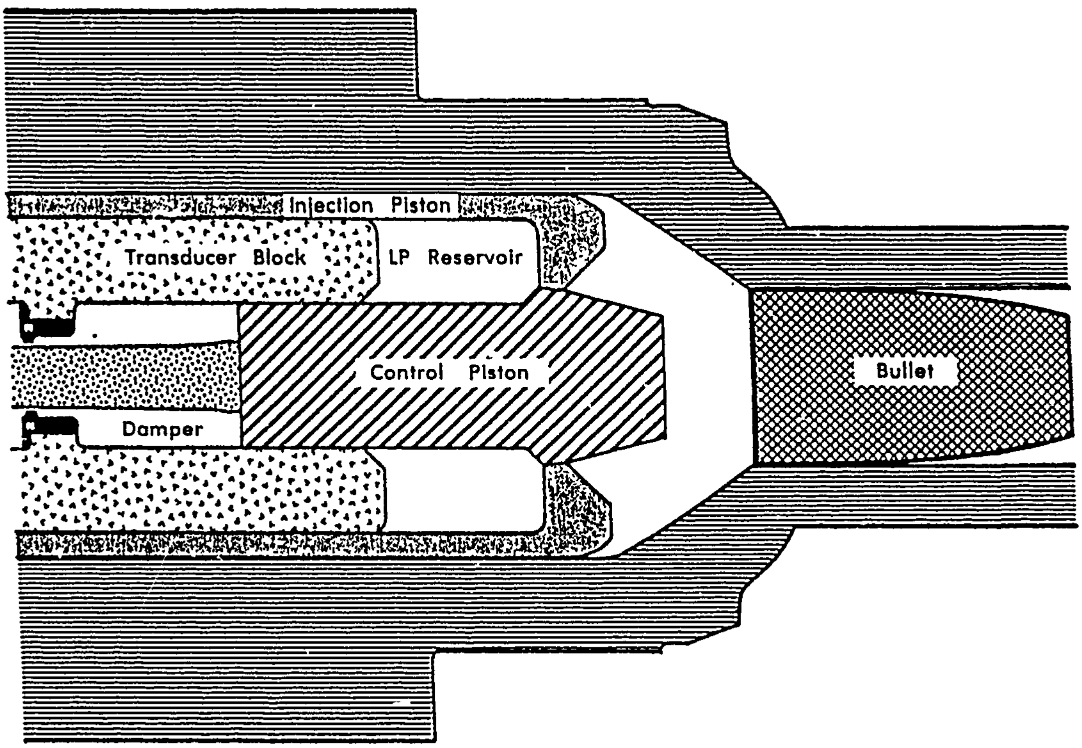

Figure 2. A Concept VIC regenerative liquid propellant gun.

The liquid jet encounters a hot, dense, and turbulent high-pressure environment of reacted and partially reacted products. Subsequently, the injected liquid undergoes an intricate series of processes, including atomization, heating, vaporization, diffusion, turbulent mixing, and chemical reaction. The details of propellant breakup and combustion are poorly understood at present, although diagnostic research efforts are ongoing to characterize the jet under gun conditions (Birk 1991). The ensuing combustion process is characterized by pressure fluctuations which typically initiate at approximately 50 MPa (Figure 1).

Several theories have been advanced for the origin of the pressure oscillations, and several are under active study. One potential explanation which has been successfully modeled maintains that the pressure fluctuations result from the combination of a highly pressure-sensitive burn rate of the propellant combined with a continuous accumulation of unburned propellant near the injector (Oberle and Wren 1991; Coffee 1992; McBratney, Teague, and Vanderhoff 1992). Another explanation advanced is that flow conditions created by the liquid jet as it emerges from the injector into the combustion chamber form vortical structures containing propellant which circulate in-phase with pressure waves and periodically release heat in the combustion chamber (Schadow 1992). A third explanation proposed is that pressure variations moving over the intact jet core result in enhanced breakup at the jet boundaries, leading to atomization and local high-energy release rates (Faeth 1992). A fourth possible source is random, impulsive combustion of ligaments of propellant in localized regions of the combustion chamber (Haberl 1991).

Visualization of the liquid propellant LGP1846 at gun conditions has not precisely determined the mechanism which initiates pressure oscillations. Diagnostics at pressures up to 30 MPa show a highly turbulent process in which flame is visible at various locations in the combustion chamber and conditions which change rapidly with time (Birk 1991). There does not appear to be an identifiable pattern to either the location or the change of location of burning. Thus, it might be conjectured the pressure fluctuations are caused by randomness in the jet breakup and energy release, resulting from one, or a combination of the mechanisms discussed above, together with mechanisms not identified.

Thus, the objective of this work is to (1) develop a physically supportable model of random energy release in the RLPG using experimental data to suggest needed parameter values in a one-dimensional (1-D) model; (2) determine to what extent the experimental pressure history can be explained by randomness in the energy release of the liquid propellant in the jet; and (3) examine the propagation of chamber pressure fluctuations from the combustion chamber to the projectiles's base in a one-dimensional (1-D) model. In addition, the model is used to suggest methods of reduction of pressure fluctuations.

2. DESCRIPTION OF MODEL

As reported previously (Wren and Gough 1990), the model is a fully 1-D continuum model of the RLPG, including treatment of the liquid reservoir, damper, combustion chamber, and tube. The governing equations for the combustion chamber are the same as those of the tube. In the general case when droplets are present, they consist of 1-D balances of mass, momentum, and energy for the mixture of combustion gases and droplets. The cross-sectional area of the flow in each of the regions of the combustion chamber or tube is that of the chamber or tube reduced by the cross-sectional area of the jet. The change in area is also considered due to the intrusion of the center bolt.

The liquid jet in the RLPG is "thick" (up to a hydraulic diameter of 1.5 cm as calculated by simulation). Breakup of the jet entails finite rate processes, and there appears to be a "conditioning time" before combustion involving atomization, heating, kinetics, etc. (Birk and Reeves 1987; Klein 1990; Bracco 1986). Attempts to apply sensitive time lag theory to the jet breakup (Coffee et al. 1991) have been successful. Sensitive time lag theory was developed as a description of the delay in energy release in liquid propellant rockets (Crocco and Cheng 1956). Sensitive time lag theory is essentially a model of energy release as a two-part step function. The first step is a conditioning time, which is related to pressure, for an injected packet of liquid. The second step is an instantaneous release of energy in the packet of liquid. Thus, it is implicitly assumed that all delay processes can be related to pressure.

The model described in this report develops a description of the jet breakup based on a conditioning time, a randomness associated with the condition of "packets" of liquid, and a Taylor theory (Birk and Bliesener 1991) which has been used to describe the energy release of liquid propellant (LP) in a limited regime.

The conditions under which the jet is injected change with time during the interior ballistic (IB) process in terms of pressures, jet velocity, etc. Physically, these changes do not take place instantaneously but occur over a finite time interval. Therefore, injection conditions would be expected to be similar over some time interval. The "coherence interval" is therefore defined in the model as the time interval over which injection conditions are expected to be similar.

However, injected propellant cannot persist indefinitely in the combustion chamber. This implies a maximum "conditioning time" before the propellant begins to release energy. The "conditioning time"

is defined as the delay time after injection before which an increment of propellant begins to release energy. The "maximum conditioning time" and the "coherence interval" are parameters which are input (fixed) at the beginning of a calculation and are illustrated in Figure 3. Since, physically, randomness in the injection of propellant is introduced into the gun by mechanical motion of the pistons, a constantly varying area for propellant flow between the two pistons, and pressure fluctuations in the liquid reservoir, as well as the breakup process, the conditioning time for the increments of propellant contained in a given coherence interval is randomly chosen to be between zero and the maximum conditioning time.

Once mature, the energy release rate of each packet of liquid is modeled with a Taylor formulation in which the breakup time is determined from entrance conditions at the interface between the liquid reservoir and the combustion chamber (Birk and Bliesener 1991). Taylor's theory is an aerodynamic theory which treats the primary atomization of the jet. The theory utilizes a parameter B which is the ratio of the Reynold's number to the Weber number, that is,

$$B = \frac{Re}{We} = \frac{\rho V D/\mu}{\rho V^2 D/\sigma} = \frac{\sigma}{\mu V},$$

with μ the viscosity, σ the surface tension, ρ the density, V the velocity, and D the diameter of the injector. In the case of an annulus, the diameter D is taken to be twice the gap or the thickness.

Thus, it is assumed that the rate of decomposition of a jet increment, once begun, is fixed by the conditions which prevail on average during the sampling interval. Each elementary increment follows an inertial trajectory which is uncoupled from that of any other increment. If the increment impacts the face of the chamber, it is partially reflected and partially transmitted to the tube according to a fixed value of admittance which is set by the user. Similarly, the velocity achieved following reflection from either the chamber face or the projectile base is related to the incident velocity by means of a user-defined coefficient of restitution. Thus, as the solution evolves, there is an aggregate of elementary jet increments, each moving inertially, except as modified by reflections from the chamber face, the projectile base and the piston face.

The assumption that each jet increment follows a purely inertial path is thought to be a reasonable first approximation, provided that the fraction of the available cross section occupied by the jet is not too large.

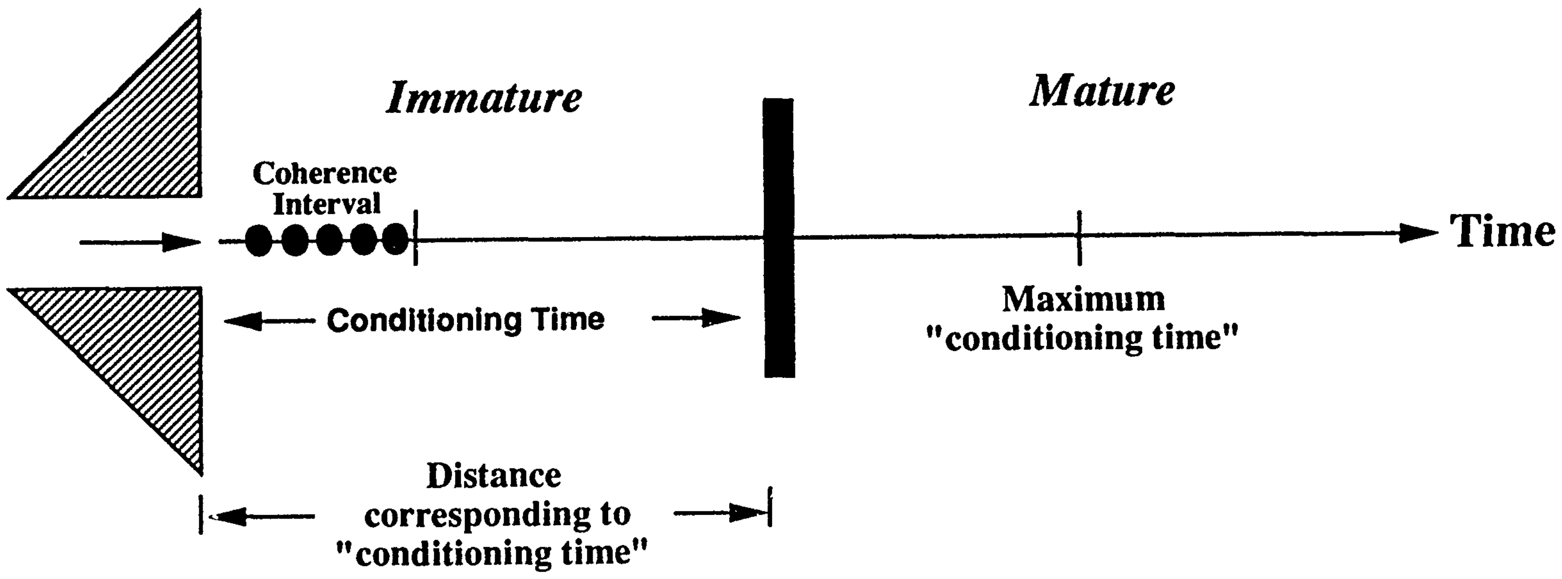

Figure 3. Illustration of "maximum conditioning time" and "coherence interval".

Considering the jet from a continuum perspective, it is radially unconfined. Accordingly, since the jet is much less compressible than the surrounding mixture, it is expected that the axial pressure distribution within the jet is controlled by the dynamics of the mixture. As one portion of the jet presses against another, it is expected that the radial boundary will displace to accommodate the interaction. Only when the jet begins to fill the cross section does this assumption break down, making it necessary to consider an axial stress field in the jet independently of that in the mixture. As for the gas dynamic forces, there are two kinds—namely, drag and buoyancy. Drag forces are expected to exert a negligible influence on the momentum of the jet; the associated shear is accommodated by the material which is converted to droplets. The buoyancy force is simply that due to gradients of the gas pressure. Although the gas pressure gradient can become large, especially at the entrance to the tube, neglect of its influence on the jet is thought to be justified at this stage of the development of the model since the density of the jet is much greater than that of the gas. The effects of buoyancy and of the stresses due to interactions between jet increments can be modeled when future applications of the code so demand.

3. MESH INDIFFERENCE

A Macormack scheme is utilized to numerically solve the governing equations. A comparison of the chamber pressure and base pressure histories for two mesh spacings are shown in Figures 4 and 5. The pressures are taken at the breech, considered to be the face of the outer piston in the combustion chamber. The solid line in Figures 4 and 5 is the solution using 33 mesh points, while the dotted line utilizes 69 mesh points in the chamber. In both cases, 21 mesh points are used in the barrel. The initial axial distance in the chamber from the piston face in the combustion chamber to the projectile base is 15.808 cm, and the final axial distance in the combustion chamber is 25.9 cm. Thus, 33 mesh points correspond to an initial spacing of 0.49 cm and a final spacing of 0.81 cm. Similarly, 69 mesh points correspond to an initial spacing of 0.23 cm and a final spacing of 0.38 cm. As can be seen from Figures 4 and 5, the solutions show some expected variation with mesh spacing. However, the details of the fluctuations from mean pressure are almost identical for either mesh spacing, and the solutions in Figures 4 and 5 demonstrate acceptable mesh indifference.

A second numeric parameter is the ratio of an elementary jet increment to the mesh spacing in the combustion chamber, referred to as BUKLEN. The solutions in terms of chamber pressure history at the breech for BUKLEN values of 0.2 (line) and 1.0 (dot) are shown in Figure 6. As can be seen in Figure 6, the solution also demonstrates reasonable insensitivity to the value of BUKLEN. Thus, the solution is felt to have demonstrated the required numeric insensitivity.

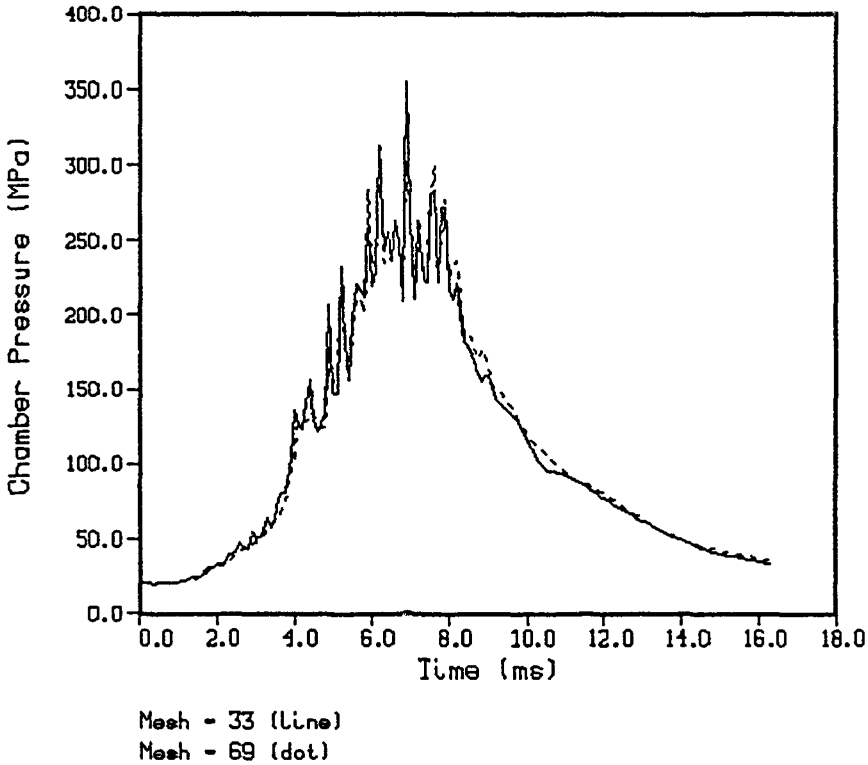

Figure 4. Comparison of breech pressure histories for 33 (line) and 69 (dot) mesh points in the chamber.

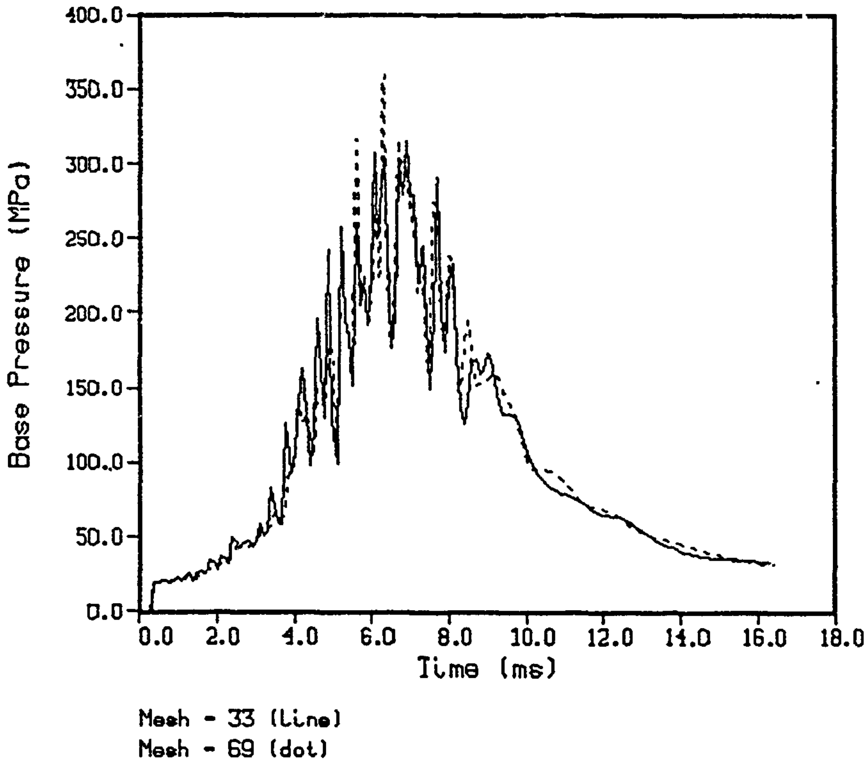

Figure 5. Comparison of projectile base pressure histories for 33 (line) and 69 (dot) mesh points in the chamber.

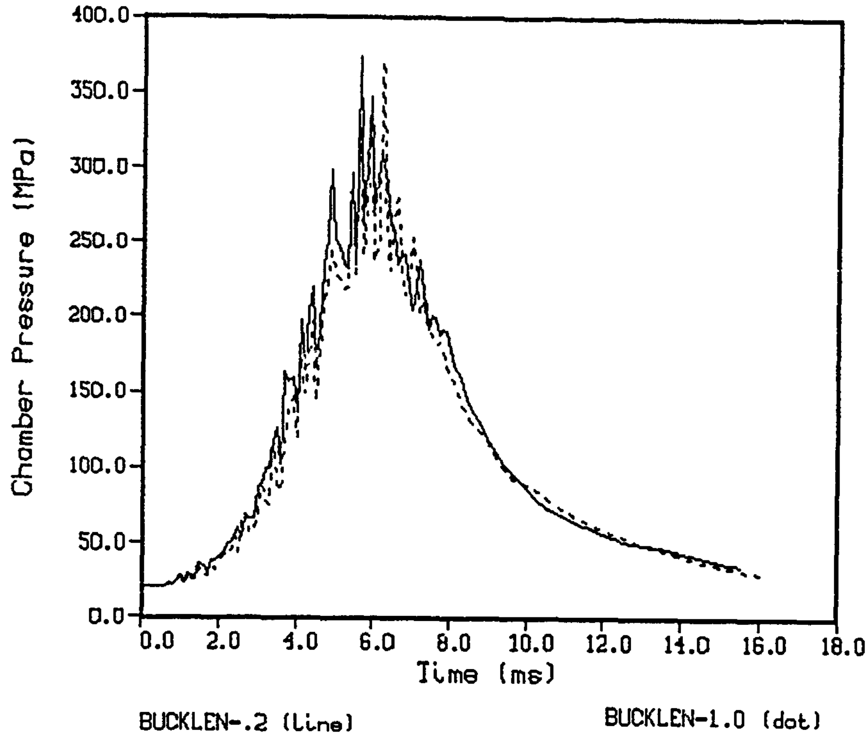

Figure 6. Comparison of breech chamber pressure histories for BUKLEN values of 0.2 (line) and 1.0 (dot).

4. APPLICATION

The model is applied to a 155-mm gun geometry. A typical experimental pressure history in the combustion chamber for a 5-liter shot, Round 81, from the first-generation gun is shown in Figure 1. An inverse analysis of the experimental data based on an energy balance yields an approximation of the liquid accumulation (liquid propellant which has been injected into the chamber but has not apparently released energy) in the combustion chamber as a function of time (Coffee, private communication 1991) as shown in Figure 7. The maximum amount of accumulated liquid propellant is estimated to be 200–400 g, depending upon the burn rate law used for the propellant (Coffee et al. 1991). The percentage of accumulation is defined as the mass of accumulated liquid propellant divided by the amount of mass injected by that time step. Accumulation has been as high as 30% in some fixtures, implying a substantial amount of unburned liquid in the combustion chamber, particularly during early times in the ballistic cycle.

In the model, the value of maximum conditioning time is chosen such that the model agrees with the approximation of the mass of accumulated liquid as shown in Figure 7. The maximum conditioning time used is 0.2 ms, the coherence interval is 0.1 ms, and the user-specified coefficient in the Taylor theory is 0.2. The resultant pressure-time simulation in the combustion chamber is shown in Figure 8. At 3 ms,

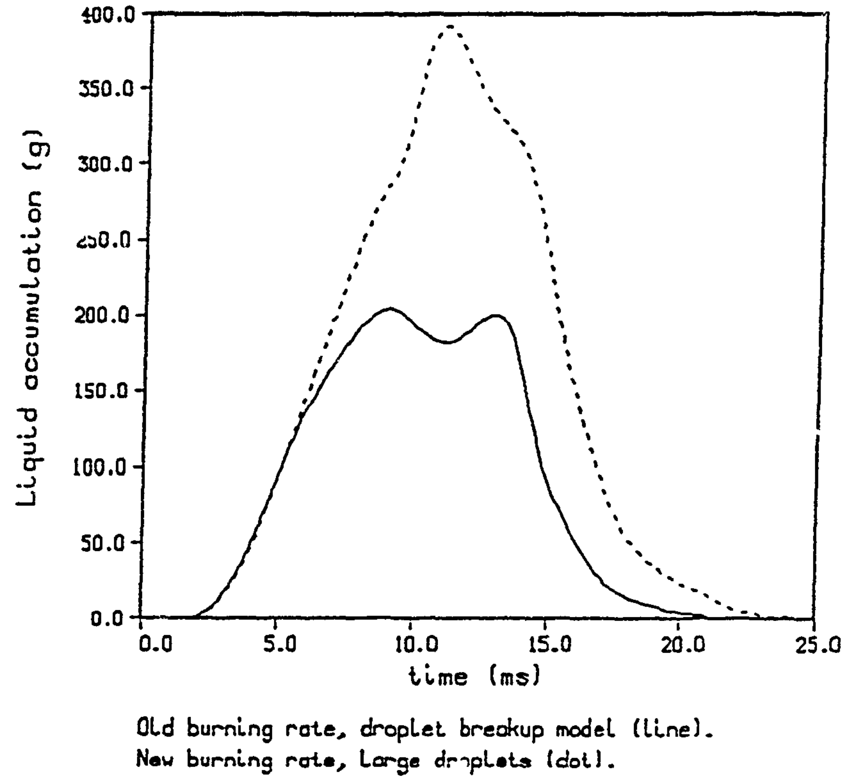

Figure 7. Liquid accumulation in the combustion chamber based on simulation.

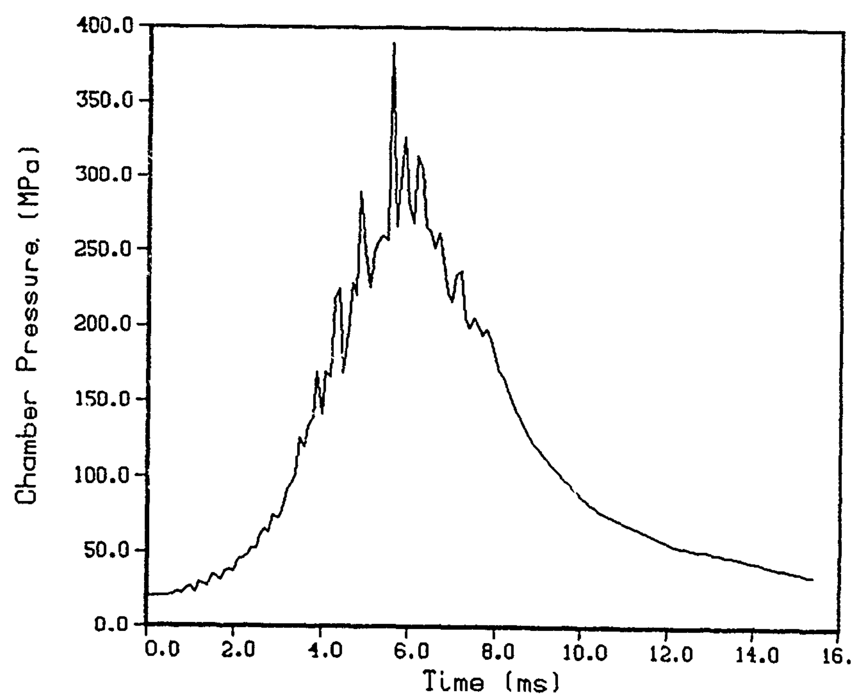

Figure 8. Simulation of chamber pressure with random breakup of liquid jet.

the injection rate is 951,692 g/s in the simulation. The coherence interval of 0.1 ms implies that approximately 95 g of liquid act as a body of fluid which translates to a distance equal to approximately the injection velocity times the coherence interval before releasing energy. The choice of the Taylor parameter is such as to induce very rapid decomposition of the fluid element once it is "mature". It is the combination of localization and rapid energy release which drives the oscillations in the present model. It can be seen that significant excursions from mean pressure can result from randomness in the jet breakup length. Since analysis of experimental data suggest radial modes in the combustion chamber, it is not expected that a 1-D model will duplicate experimental pressure histories. However, the model suggests that randomness in the jet breakup may be implicated in the production of pressure fluctuations.

A characterization of the jet at various time steps is shown in Figure 9, where 0.0 cm represents the tube origin and −15.8 cm represents the initial piston position. At each timestep shown, the location and amount of mass in the jet is shown, with the right-most boundary representing the face of the piston. Since the piston is moving rearward to inject liquid propellant, the right-most boundary recedes with time. It is noted that, consistent with the derived accumulation from experiment, the jet is short. Even with little penetration into the combustion chamber, the liquid jet provides an energy source for substantial pressure fluctuations. The base pressure history for this simulation is shown in Figure 10. It can be seen that the fluctuations in chamber pressure propagate acoustically to the base of the projectile and that substantial fluctuations in the base pressure result. The model, therefore, validates observations of downbore pressure histories which exhibit oscillations of similar amplitude to those measured in the combustion chamber. Since the modeled jet is quite short and the chemical energy release is confined to the combustion chamber, the pressure oscillations at the projectile base are shown to be a consequence of 1-D wave propagation rather than local energy release at the projectile base. However, it is noted that a 1-D model is not capable of describing possible three-dimensional effects which could randomize the pressure fluctuations on the base of the projectile, an issue of interest to the munitions community.

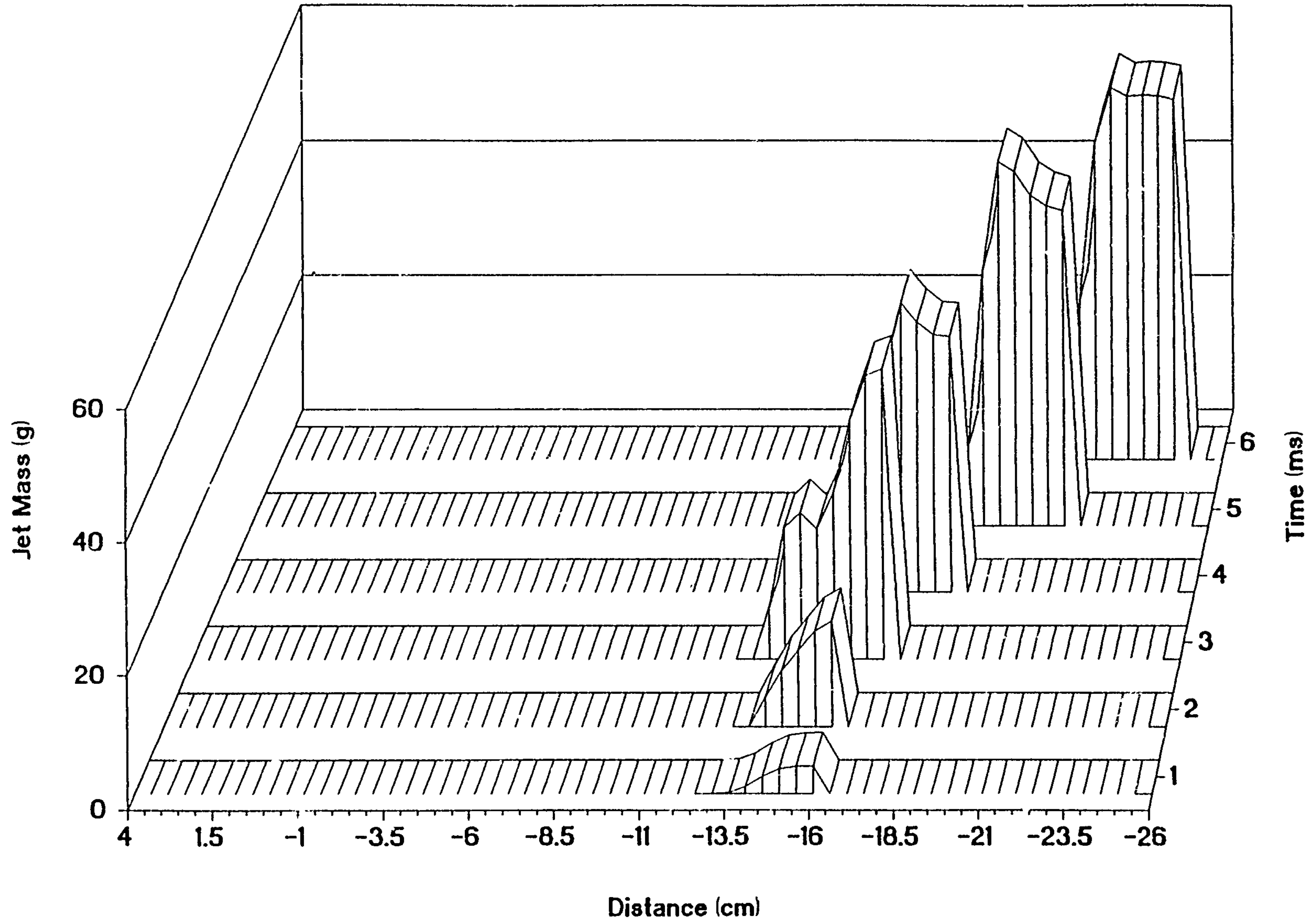

Figure 9. Mass in the jet at various time steps based on simulation.

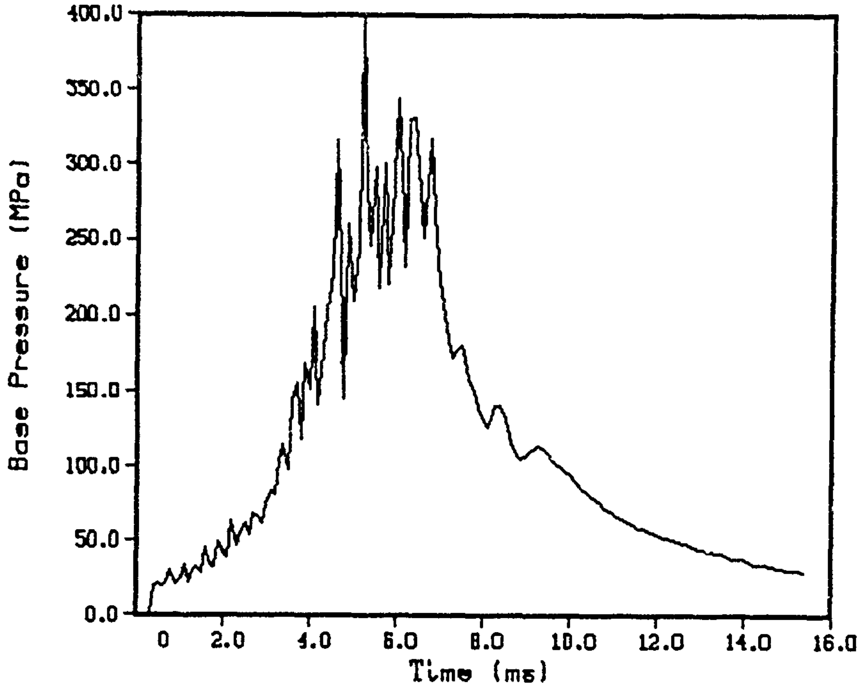

Figure 10. Simulation of base pressure history with random jet breakup.

5. REDUCTION OF PRESSURE OSCILLATIONS

In this theoretical study, pressure fluctuations can be reduced by decreasing the maximum conditioning time or decreasing the coherence interval or both. However, since the initial conditions are not changed, it is more physically meaningful to utilize the same value of the coherence interval. Thus, the maximum conditioning time is decreased. In Figure 11, the jet breakup is random, but the maximum conditioning time is 1/10 the previous value used in Figure 8. The maximum conditioning time used is 0.02 ms, the coherence interval is 0.1 ms, and the user-specified coefficient in the Taylor theory is 0.2. At a similar injection velocity at 3 ms, compared to the previous simulation, a maximum conditioning time of 0.02 ms implies that the jet increment will begin releasing energy almost immediately upon introduction into the combustion chamber.

The results suggest that injection patterns which break the liquid propellant into small packets, such as finely atomized sprays or jet splitters, may result in quieter combustion. Jet splitters have been successfully utilized in a diagnostic LP fixture (Rychanovsky 1991) and in a 30-mm gun (Despirito 1991). Jet splitters are mounted downstream of the injector and are intended to disrupt the liquid jet. Currently

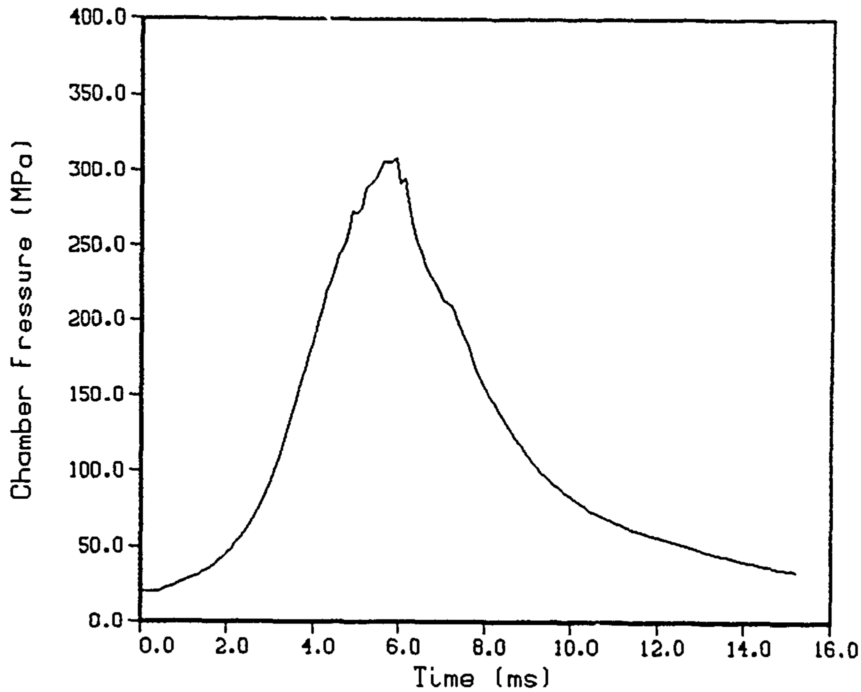

Figure 11. Simulation of chamber pressure history reducing the degree of coherence in the jet breakup.

they have achieved only limited success in reducing pressure oscillations. However, the model suggests that mechanisms which shorten the time from injection to the beginning of energy release may reduce pressure oscillations.

6. SUMMARY

A one-dimensional model of the regenerative liquid propellant gun has been presented which uses a Taylor theory for the breakup and energy release of the liquid jet and treats the axial extension of the jet in the combustion chamber. The model allows for randomness in the jet breakup to mimic the physical conditions of randomness in conditioning time which may be associated with propellant combustion. The model suggests that:

(1) significant fluctuations in chamber pressure can be produced with a random jet breakup length, even with short jets;

(2) if pressure oscillations are due to rough combustion, energy can be radiated acoustically to the base of the projectile;

(3) downbore pressure fluctuations are physically plausible, even with short jets confined to the combustion chamber;

(4) pressure fluctuations can be potentially reduced by decreasing the conditioning time before the liquid propellant begins to release energy.

One interpretation of conclusion (4) is to finely atomize the liquid or break it apart upon introduction into the chamber. This analysis suggests that designs which utilize thicker jets in order to increase the mass flow into the combustion chamber may be expected to experience even larger magnitudes in the amplitude of pressure oscillations due to the potential for more coherence in the structure of the jet.

INTENTIONALLY LEFT BLANK.

7. REFERENCES

Bannister, K., T. Coffee, G. Wren, and S. Wilkerson. "Finite Element Analyses of 155-mm Projectile Response to LP-Type Loading." Paper presented at the 28th JANNAF Combustion Meeting, Brooks Air Force Base, San Antonio, TX, October 1991.

Birk, A., and P. Reeves. "Annular Liquid Propellant Jets-Injection, Atomization and Ignition." BRL-TR-2780, U.S. Army Ballistic Research Laboratory, Aberdeen Proving Ground, MD, March 1987.

Birk, A., and G. Bliesener. "Comparative Spray Reactivities of LGP 1845/98 and Their Subcomponents." Proceedings of the 28th JANNAF Combustion Meeting, San Antonio, TX, October 1991.

Bracco, F. "High Pressure Injection of Liquid Sprays." Published in ARO/BRL/JANNAF Workshop Summary Report, "Injection and Combustion of Liquid Monopropellants in a Regenerative Liquid Propellant Gun." Edited by D. Mann, G. Wren, and A. Mellor, 9–10 October 1986.

Carling, R., R. Rychnovsky, S. Griffiths, S. Vosen, and R. Renzi. "Progress Report on Reduction of Pressure Oscillations in the Liquid Propellant Injector/Combustor." Proceedings of the 28th JANNAF Combustion Subcommittee Meeting, vol. III, San Antonio, TX, October 1991.

Coffee, T. P., G. P. Wren, and W. F. Morrison. "A Comparison Between Experiment and Simulation for Concept VIC Regenerative Liquid Propellant Guns. I. 30 mm." BRL-TR-3072, U.S. Army Ballistic Research Laboratory, Aberdeen Proving Ground, MD, December 1989.

Coffee, T. P., G. P. Wren, and W. F. Morrison. "A Comparison Between Experiment and Simulation for Concept VIC Regenerative Liquid Propellant Guns. II. 105 mm." BRL-TR-3093, U.S. Army Ballistic Research Laboratory, Aberdeen Proving Ground, MD, March 1990.

Coffee, T. P., P. Baer, W. F. Morrison, and G. P. Wren. "Jet Breakup and Combustion Modeling for the Regenerative Liquid Propellant Gun." BRL-TR-3223, U.S. Army Ballistic Research Laboratory, Aberdeen Proving Ground, MD, April 1991.

Coffee, T. Private communication. U.S. Army Ballistic Research Laboratory, Aberdeen Proving Ground, MD, 1991.

Coffee, T. "A Two-Dimensional Model for the Combustion Chamber/Gun Tube of a Concept VIC Regenerative Liquid Propellant Gun." BRL-TR-3341, U.S. Army Ballistic Research Laboratory, Aberdeen Proving Ground, MD, May 1992.

Cook, G. Private communication. RARDE Fort Halstead, England, 1990.

Crocco, L., and S. Cheng. Theory of Combustion Instability in Liquid Propellant Rocket Motors. Butterworths Scientific Publications, 1956.

Despirito, J., N. Boyer, J. Knapton, and A. Johnson. "Pressure Oscillation Reduction in a 30 mm Concept VIC RLPG." Proceedings of the 28th JANNAF Combustion Subcommittee Meeting, vol. I, San Antonio, TX, October 1991.

Faeth, G. Private communication. University of Michigan, 1992.

Haberl, B. Private communication, General Electric Company, 1991.

Klein, N. "Ignition and Combustion of the HAN-Based Liquid Propellants." Proceedings of the 27th JANNAF Combustion Meeting, Cheyenne, WY, October 1990.

Klingenberg, G. Private communication. Ernst Mach Institute, Germany, 1991.

McBratney, W., M. Teague, and J. Vanderhoff. Private communication. U.S. Army Research Laboratory, Aberdeen Proving Ground, MD, 1992.

Oberle, W., and Wren, G. "Burn Rates of LGP 1846 Conditioned Ambient, Hot, and Cold." BRL-TR-3287, U.S. Army Ballistic Research Laboratory, Aberdeen Proving Ground, MD, October 1991.

Rychanovsky, R. Private communication. Sandia National Laboratories, 1991.

Schadow, K. Private communication. China Lake, CA, 1992.

Wren, G. P., T. P. Coffee, and W. F. Morrison. "A Comparison Between Experiment and Simulation for Concept VIC Regenerative Liquid Propellant Guns. III. 155 mm." U.S. Army Ballistic Research Laboratory, Aberdeen Proving Ground, MD, to be published.

Wren, G., and P. Gough. "A One-Dimensional Analysis of a Liquid Jet in a Regenerative Liquid Propellant Gun." BRL-TR-3077, U.S. Army Ballistic Research Laboratory, Aberdeen Proving Ground, MD, April 1990.

APPENDIX:

OUTPUT FROM COMPUTER SIMULATION

INTENTIONALLY LEFT BLANK.

```
    MAX TIME LIMIT set to 600 seconds
1 SIMULATION OF INTERIOR BALLISTICS OF HYBRID LIQUID PROPELLANT GUN  VERSION OF JUNE 20,
1985
          OPTION SWITCHES

 NRGEN(0=CONVENTIONAL RLPG,1=REVERSE ANNULAR)    2
      (2=CONV. COMPOUND,3=RAP COMPOUND)
 KIN1(0=INFINITE HELMHOLTZ MIXING RATE,
      1=FINITE RATE
      2=FINITE RATE,FINITE BOOSTER JET   )       2
 KIN2(0=INSTANTANEOUS DROPLET COMBUSTION,
      1=FINITE RATE)                             0
 ICP (0 - USE VENT AREA)
     (1 - COMPUTE VENT AREA FOR CONST. PRES.)
     (2 - COMPUTE VENT AREA FOR CONST. ACC.)     0
 IPAR (0 - NORMAL INPUT)
      (1 - COMPUTE LIQUID & COMBUSTION VOLUMES)
      (2 - COMPUTE LIQUID VOLUME FROM C/M)       0
 NHTW (0 - WALL TEMP. NOT UPDATED
      (1 - WALL TEMP. UPDATED)                   0
 JHTW (0 - NO HEAT LOSS)
      (1 - HEAT LOSS TO TUBE)                    1
 NTEM (NO. OF TUBE INITIAL TEMP. PROFILE ENTRIES 0
 NENV (NO. OF TUBE INTERVALS FOR PRESS ENVELOPE) 0
 NPISR (0 - NO PISTON RESISTANCE
     (1 - PISTON RESISTANCE FUNCTION OF TRAVEL
     (2 - PISTON RESISTANCE FUNCTION OF VELOCITY  0
 NCD (0 - CD IS CONSTANT)
     (1 - CD IS FUNCTION OF PISTON TRAVEL)        0
 NORVS (0 - NO BACKFLOW TO LP BOOSTER CHAMBER)
       (1 - BACKFLOW IS ALLOWED)                  0
 IGNITR (0 - BOOSTER IGNITER NOT MODELED)
        (1 - BOOSTER IGNITER IS MODELED)          0
 IGNLOC (0 - BOOSTER IGNITER NOT ON SIDEWALL)
        (1 - BOOSTER IGNITER IS ON SIDEWALL)      0
 NXPEL  (0 - TC EXPULSION CHARGE NOT PRESENT)
        (1 - TC EXPULSION CHARGE IS PRESENT)      0
 NARB   (0 - VENT GEOMETRY NOT PRESCRIBED BY ARBV 0)
        (1 - VENT GEOMETRY SPECIFIED BY ARBVEN)
```

```
          LOGOUT PARAMETERS

SAVE ON UNIT 8(0=NO,1=YES)                                  0
START FROM UNIT 8(0=NO,>0=STEP TO START)                    0
PLOTTING ON LOGOUT(0=NO,1=YES)                              1
NUMBER OF STEPS BEFORE LOGOUT                            9999
TIME INTERVAL BEFORE LOGOUT(MSEC)                             0.100
DEBUG PRINT REQUIRED (0=NO,1=YES)                           0
INPUT DATA PRINTED (Y=0,N=1)                                0
TRAJECTORY DATA PRINTED (Y=0,N=1)                           0
EXTRA TRAJECTORY DATA PRINTED (Y=0,N=1)                    0
MASS BAL. REG 1>4 DATA PRINTED (Y=0,N=1)                   0
MASS BAL. REG 5>8 DATA PRINTED (Y=0,N=1)                   0
ENERGY BAL. REG 1>4 DATA PRINTED (Y=0,N=1)                 0
ENERGY BAL. REG 1>4 (CONT) DATA PRINTED (Y=0,N=1) 0
ENERGY BAL. REG 5>8 DATA PRINTED (Y=0,N=1)                 0
PROFILE AND PLOT DATA PRINTED (Y=0,N=1)                     0

          TERMINATION PARAMETERS

NUMBER OF INTEGRATION STEPS                             99999
TIME INTERVAL(MSEC)                                       100.000
PROJECTILE TRAVEL(CM)                                     591.800


          INTEGRATION PARAMETERS

NUMBER OF POINTS ASSIGNED TO TRAVELING CHARGE       0
MAXIMUM NUMBER OF POINTS ASSIGNED TO TUBE          21
MINIMUM MESH SPACING IN TRAVELING CHARGE(CM)          0.500
MINIMUM MESH SPACING IN TUBE(CM)                      0.100
C-F-L SAFETY FACTOR(-)                                3.000
FLUX CONVERGENCE TOLERANCE(GM**2/SEC**2)              0.010
SOURCE TERM STABILITY FACTOR(-)                       0.050


MAXIMUM NUMBER OF MESH POINTS ASSIGNED TO EACH CHAMBER     33
MINIMUM MESH SPACING IN RESERVOIR(CM)                    0.200
```

DESCRIPTION OF TUBE

NUMBER OF PAIRS OF OBTURATOR RESISTANCE DATA	4
AIR SHOCK RESISTANCE(0=NO,1=YES)	1
TUBE DIAMETER(CM)	15.500
TUBE ENTRANCE COEFFICIENT(-)	1.000

OBTURATOR RESISTANCE

PROJECTILE TRAVEL(CM)	RESISTANCE(MPA)
0.000	10.000
3.810	10.000
4.000	3.000
591.800	3.000

PROPERTIES OF GAS IN FRONT OF PROJECTILE

INITIAL PRESSURE(MPA)	0.100
INITIAL TEMPERATURE(DEG.K)	300.000
RATIO OF SPECIFIC HEATS(-)	1.400
MOLECULAR WEIGHT(GM/GMOL)	28.840

PROPERTIES OF PROJECTILE

MASS(GM)	43200.000
LOCATION OF BASE WITH RESPECT TO TUBE ENTRANCE(CM)	0.000
TRAVEL REQUIRED TO INITIATE VENTING OF TRAVELING LIQUID CHARGE(CM)	0.000
DENSITY OF AFTERBODY MATERIAL(GM/CC)	0.000
PRESSURE FOR SEPARATION OF TLC FROM BASE OF PROJECTILE(MPA)	0.000

PROPERTIES OF COMPOUND RLPG BOOSTER

INITIAL VOLUME OF FUEL CHAMBER(CC)	5204.860
INITIAL VOLUME OF COMBUSTION CHAMBER(CC)	8406.000
INJECTION HOLE AREA(CM**2)	53.600
NUMBER OF INJECTION HOLES(-)	1.000
INJECTION HOLE DISCHARGE COEFFICIENT(-)	0.950

PROPERTIES OF FORWARD CYLINDER

MASS OF PISTON(GM)	109000.000
INITIAL VOLUME OF DAMPING LIQUID CHAMBER(CC)	0.000
VOLUME OF D.L. RECEIVER CHAMBER(CC)	0.000
FUEL SIDE PISTON AREA(CM**2)	461.511
COMBUSTION CHAMBER SIDE PISTON AREA(CM**2)	661.864
DAMPING CHAMBER SIDE PISTON AREA(CM**2)	0.000
MAXIMUM PISTON DISPLACEMENT(CM)	10.104
% OF MAXIMUM PISTON DISPLACEMENT	0.980

PROPERTIES OF CENTER CYLINDER

MASS OF PISTON(GM)	0.000
INITIAL VOLUME OF DAMPING LIQUID CHAMBER(CC)	0.000
VOLUME OF D.L. RECEIVER CHAMBER(CC)	0.000
FUEL SIDE PISTON AREA(CM**2)	0.000
COMBUSTION CHAMBER SIDE PISTON AREA(CM**2)	0.000
DAMPING CHAMBER SIDE PISTON AREA(CM**2)	0.000
MAXIMUM PISTON DISPLACEMENT(CM)	0.000
% OF MAXIMUM PISTON DISPLACEMENT	0.000

PROPERTIES OF REAR CYLINDER

MASS OF PISTON(GM)	0.000
INITIAL VOLUME OF DAMPING LIQUID CHAMBER(CC)	0.000
VOLUME OF D.L. RECEIVER CHAMBER(CC)	0.000
FUEL SIDE PISTON AREA(CM**2)	0.000
COMBUSTION CHAMBER SIDE PISTON AREA(CM**2)	0.000
DAMPING CHAMBER SIDE PISTON AREA(CM**2)	0.000
MAXIMUM PISTON DISPLACEMENT(CM)	0.000
% OF MAXIMUM PISTON DISPLACEMENT	0.000

```
1          GEOMETRIC DATA FOR CONTINUUM ANALYSIS OF CHAMBERS

 DIST. FROM TUBE TO FORWARD CYLINDER(CM)                      15.808
 DIST. FROM TUBE TO CENTER CYLINDER(CM)                       12.808
 DIST. FROM TUBE TO REAR CYLINDER(CM)                         25.912
 DIST. FROM TUBE TO REAR OF INT. CHAMBER(CM)                   0.000
 DIST. FROM TUBE TO BREECH(CM)                                 0.000
 LENGTH OF INJECTION HOLES IN FWD. CYL.(CM)                    0.000

0     DIST. FROM TUBE(CM)     RADIUS OF C.C.(CM)

            0.00000                 7.7500
             13.691                 16.497
             30.000                 16.497
0     DIST. FROM FRONT(CM)     RADIUS OF FWD. CYL.(CM)

            0.00000                 14.435
             30.000                 14.435
0     DIST. FROM FRONT(CM)     RADIUS OF CENT. CYL.(CM)

            0.00000                0.00000
             3.0000                 6.6650
             33.000                 6.6650

          PROPERTIES OF DAMPING LIQUID

 DENSITY AT ONE ATMOSPHERE(GM/CC)                      0.889
 BULK MODULUS AT ONE ATMOSPHERE(MPA)                1600.000
 DERIVATIVE OF MODULUS W.R.T PRESSURE(-)              11.300

          COMPOUND BOOSTER CONTROL DATA

 NPXSGN (0 - FUEL INJECTION AREA GIVEN AS FUNCTION OF
             Z-FWD MINUS Z-CENTER)                   0
        (1 - FUEL INJECTION AREA GIVEN AS FUNCTION OF
             Z-CENTER MINUS Z-FWD)
 NO. OF DATA TO DESCRIBE FWD CYL DAMPER VENT AREA            0
 NO. OF DATA TO DESCRIBE CENTER CYL DAMPER VENT AREA         0
 NO. OF DATA TO DESCRIBE REAR CYL DAMPER VENT AREA           0
```

```
NO. OF DATA TO DESCRIBE FWD CYL DAMPER DISCHARGE COEFF               0
NO. OF DATA TO DESCRIBE CENTER CYL DAMPER DISCHARGE COEFF            0
NO. OF DATA TO DESCRIBE REAR CYL DAMPER DISCHARGE COEFF              0
NPISRC(1) (0 - NO RESISTANCE FOR FWD CYL)          0
          (1 - RES. DEPENDS ON DISP.)
          (2 - RES. DEPENDS ON VEL. AND PRES.)
          (3 - COMBINATION OF 1 AND 2)
NPISRC(2) - RESISTANCE LAW FOR CENTER CYL          0
NPISRC(3) - RESISTANCE LAW FOR REAR CYL            0
NSIDEV (0 - RAP INJECTION AS ABOVE)                0
       (>0 - NUMBER OF SIDEWALL VENTING DATA)

          PROPERTIES OF LIQUID FUEL

DENSITY AT ONE ATMOSPHERE(GM/CC)                      1.430
BULK MODULUS AT ONE ATMOSPHERE(MPA)                5350.000
DERIVATIVE OF MODULUS W.R.T PRESSURE(-)               9.110
CHEMICAL ENERGY(J/GM)                              4035.500
RATIO OF SPECIFIC HEATS OF PRODUCTS(-)                1.223
MOLECULAR WEIGHT OF PRODUCTS(GM/GMOL)                22.848
COVOLUME OF PRODUCTS(CC/GM)                           0.677

          FINITE RATE HELMHOLTZ MIXING DATA

DROPLET DIAMETER(CM)                                  0.001
HELMHOLTZ MIXING COEFFICIENT(GM/CM)                   0.000

      BOOSTER JET PROPERTIES

BREAKUP LENGTH COEFFICIENT(-)                       0.200
SURFACE TENSION(GM/SEC**2)                          0.000
VISCOSITY(GM/CM-SEC)                                20.000
NOZZLE INVERSE AREA INTEGRAL(1/CM)                  0.000
COEFFICIENT OF RESTITUTION FOR JET IMPACT(-)        1.000
TUBE ADMITTANCE(-)                                  1.000
INCREMENT LENGTH/MESH SPACING(-)                    0.200
MAXIMUM DELAY FOR START OF BREAKUP(MSEC)            0.200
AUTOCORRELATION TIME(MSEC)                          0.100
INTERVAL FOR WRITE TO UNIT 24(MSEC)                 0.100
```

INITIAL DATA

PRESSURE OF GAS(MPA)	20.000
PRESSURE OF LIQUID BOOSTER CHARGE(MPA)	3.450
PRESSURE OF LIQUID TRAVELING CHARGE(MPA)	0.000
TEMPERATURE(DEG.K)	2569.000
PRESSURE OF DAMPING LIQUID(MPA)	3.450

DESCRIPTION OF INITIAL CAVITY

NUMBER OF PAIRS OF DATA TO DESCRIBE CAVITY	0
CAVITY MECHANICALLY STABILIZED(0=NO,1=YES)	1

CROSS-SECTIONAL AREA COMBUSTION CHAMBER(CM**2) 855.019

PISTON TRAVEL - INJECTION AREA TABLE

F. PISTON TRAVEL	PISTON TRAVEL(CM)	VENT AREA (CM**2)
0.0000	0.000	0.100000E-01
0.1000	1.016	53.6000
1.0000	10.156	53.6000

THERMAL PROPERTIES OF TUBE

INITIAL TUBE TEMPERATURE (DEG.K)	300.000
THERMAL CONDUCTIVITY (J/CM-SEC-DEG.K)	0.622100
THERMAL DIFFUSIVITY (CM**2/SEC)	0.147100
EMISIVITY FACTOR (-)	1.00000
HEAT LOSS MULTIPLIER FACTOR (-)	1.54000

TOTAL PROPELLANT WEIGHT (GM)	7621.474
TOTAL CHEMICAL ENERGY (KJ)	30785.07
BOOSTER WEIGHT (GM)	7447.207
TRAVELING CHARGE WEIGHT (GM)	0.0000000
IGNITER WEIGHT (GM)	177.2681
LOADING DENSITY (GM/CC)	0.5599553
C/M	0.1764230

1 LIQUID PROPELLANT GUN IB TRAJECTORY

TIME	-----------PRESSURE (MPA)-----------					TEMP. (DEG K)		----PISTON--------		--PROJECTILE-----		ACCEL	Z	F.DROP	PR4/PL4	CD	STEP
MS	LIQUID	I.CHLMBR	C.CHMBR	THROAT	BASE	CHAMBER	THROAT	POS.(CM)	VEL.(M/S)	POS.(M)	VEL(M/S)	(KG)		%		(LIQ)	
0.000	3.5	0.0	20.0	0.0	0.0	2569.	0.	0.000	0.000	0.000	0.00	0.0	0.000	0.000	1.0000	0.950	0

STEP NUMBER = 0 TIME(MSEC) = 0.000 DELTA T(MSEC) = 0.0000

PROJECTILE TRAVEL (M)	0.0000
PROJECTILE VELOCITY (M/S)	0.0000
PISTCN TRAVEL (CM)	0.0000
PISTON VELOCITY (M/S)	0.0000
UNATOMIZED FRACTION OF BOOSTER CHARGE (%)	100.000
UNATOMIZED FRACTION OF TRAVELING CHARGE (%)	0.000
FRACTION OF TOTAL FUEL IN DROPLET PHASE (%)	0.000
TOTAL MASS (GM)	7621.474
MASS DEFECT (%)	0.000
TOTAL ENERGY (J)	30785072.299
ENERGY DEFECT (%)	0.000
OBTURATOR RESISTANCE (MPA)	0.000
AIR SHOCK RESISTANCE (MPA)	0.000
MASS OF AXIAL JET(GM)	0.000
LENGTH OF AXIAL JET (CM)	0.0000
MAX. LENGTH OF AXIAL JET (CM)	0.0000
RATE OF INJECTION OF JET(GM/S)	0.000000
RATE OF DISINTEGRATION OF JET(GM/S)	0.000000
TAYLOR JET PARAMETER(-)	0.000000

REGION	MESH POINT	Z(M)	P(MPA)	RHO(GM/CC)	U(M/S)	EPS(-)	T(DEG.K)	SIGEQ(MPA)	CAV.RAD(CM)	JET MASS(GM/CM)	JET VEL(M/S)
1	1	-0.2591	3.450	1.4309	0.0000	0.0000	0.0	0.000	0.000	0.0000	0.0000
1	2	-0.2560	3.450	1.4309	0.0000	0.0000	0.0	0.000	0.000	0.0000	0.0000
1	3	-0.2528	3.450	1.4309	0.0000	0.0000	0.0	0.000	0.000	0.0000	0.0000
1	4	-0.2496	3.450	1.4309	0.0000	0.0000	0.0	0.000	0.000	0.0000	0.0000

REGION	MESH POINT	Z(M)	P(MPA)	RHO(GM/CC)	U(M/S)	EPS(-)	T(DEG.K)	SIGEQ(MPA)	CAV.RAD(CM)	JET MASS(GM/CM)	JET VEL(M/S)
1	5	-0.2465	3.450	1.4309	0.0000	0.0000	0.0	0.000	0.000	0.0000	0.0000
1	6	-0.2433	3.450	1.4309	0.0000	0.0000	0.0	0.000	0.000	0.0000	0.0000
1	7	-0.2402	3.450	1.4309	0.0000	0.0000	0.0	0.000	0.000	0.0000	0.0000
1	8	-0.2370	3.450	1.4309	0.0000	0.0000	0.0	0.000	0.000	0.0000	0.0000
1	9	-0.2339	3.450	1.4309	0.0000	0.0000	0.0	0.000	0.000	0.0000	0.0000
1	10	-0.2307	3.450	1.4309	0.0000	0.0000	0.0	0.000	0.000	0.0000	0.0000
1	11	-0.2275	3.450	1.4309	0.0000	0.0000	0.0	0.000	0.000	0.0000	0.0000
1	12	-0.2244	3.450	1.4309	0.0000	0.0000	0.0	0.000	0.000	0.0000	0.0000
1	13	-0.2212	3.450	1.4309	0.0000	0.0000	0.0	0.000	0.000	0.0000	0.0000
1	14	-0.2181	3.450	1.4309	0.0000	0.0000	0.0	0.000	0.000	0.0000	0.0000
1	15	-0.2149	3.450	1.4309	0.0000	0.0000	0.0	0.000	0.000	0.0000	0.0000
1	16	-0.2118	3.450	1.4309	0.0000	0.0000	0.0	0.000	0.000	0.0000	0.0000
1	17	-0.2086	3.450	1.4309	0.0000	0.0000	0.0	0.000	0.000	0.0000	0.0000
1	18	-0.2054	3.450	1.4309	0.0000	0.0000	0.0	0.000	0.000	0.0000	0.0000
1	19	-0.2023	3.450	1.4309	0.0000	0.0000	0.0	0.000	0.000	0.0000	0.0000
1	20	-0.1991	3.450	1.4309	0.0000	0.0000	0.0	0.000	0.000	0.0000	0.0000
1	21	-0.1960	3.450	1.4309	0.0000	0.0000	0.0	0.000	0.000	0.0000	0.0000
1	22	-0.1928	3.450	1.4309	0.0000	0.0000	0.0	0.000	0.000	0.0000	0.0000
1	23	-0.1897	3.450	1.4309	0.0000	0.0000	0.0	0.000	0.000	0.0000	0.0000
1	24	-0.1865	3.450	1.4309	0.0000	0.0000	0.0	0.000	0.000	0.0000	0.0000
1	25	-0.1833	3.450	1.4309	0.0000	0.0000	0.0	0.000	0.000	0.0000	0.0000
1	26	-0.1802	3.450	1.4309	0.0000	0.0000	0.0	0.000	0.000	0.0000	0.0000
1	27	-0.1770	3.450	1.4309	0.0000	0.0000	0.0	0.000	0.000	0.0000	0.0000
1	28	-0.1739	3.450	1.4309	0.0000	0.0000	0.0	0.000	0.000	0.0000	0.0000
1	29	-0.1707	3.450	1.4309	0.0000	0.0000	0.0	0.000	0.000	0.0000	0.0000
1	30	-0.1675	3.450	1.4309	0.0000	0.0000	0.0	0.000	0.000	0.0000	0.0000
1	31	-0.1644	3.450	1.4309	0.0000	0.0000	0.0	0.000	0.000	0.0000	0.0000
1	32	-0.1612	3.450	1.4309	0.0000	0.0000	0.0	0.000	0.000	0.0000	0.0000
1	33	-0.1581	3.450	1.4309	0.0000	0.0000	0.0	0.000	0.000	0.0000	0.0000
3	36	-0.1581	20.000	0.21088E-01	0.0000	1.0000	2569.0	0.000	0.000	0.0000	0.0000
3	37	-0.1531	20.000	0.21088E-01	0.0000	1.0000	2569.0	0.000	0.000	0.0000	0.0000
3	38	-0.1482	20.000	0.21088E-01	0.0000	1.0000	2569.0	0.000	0.000	0.0000	0.0000
3	39	-0.1433	20.000	0.21088E-01	0.0000	1.0000	2569.0	0.000	0.000	0.0000	0.0000
3	40	-0.1383	20.000	0.21088E-01	0.0000	1.0000	2569.0	0.000	0.000	0.0000	0.0000
3	41	-0.1334	20.000	0.21088E-01	0.0000	1.0000	2569.0	0.000	0.000	0.0000	0.0000
3	42	-0.1284	20.000	0.21088E-01	0.0000	1.0000	2569.0	0.000	0.000	0.0000	0.0000
3	43	-0.1235	20.000	0.21088E-01	0.0000	1.0000	2569.0	0.000	0.000	0.0000	0.0000
3	44	-0.1186	20.000	0.21088E-01	0.0000	1.0000	2569.0	0.000	0.000	0.0000	0.0000
3	45	-0.1136	20.000	0.21088E-01	0.0000	1.0000	2569.0	0.000	0.000	0.0000	0.0000
3	46	-0.1087	20.000	0.21088E-01	0.0000	1.0000	2569.0	0.000	0.000	0.0000	0.0000
3	47	-0.1037	20.000	0.21088E-01	0.0000	1.0000	2569.0	0.000	0.000	0.0000	0.0000
3	48	-0.0988	20.000	0.21088E-01	0.0000	1.0000	2569.0	0.000	0.000	0.0000	0.0000
3	49	-0.0939	20.000	0.21088E-01	0.0000	1.0000	2569.0	0.000	0.000	0.0000	0.0000
3	50	-0.0889	20.000	0.21088E-01	0.0000	1.0000	2569.0	0.000	0.000	0.0000	0.0000
3	51	-0.0840	20.000	0.21088E-01	0.0000	1.0000	2569.0	0.000	0.000	0.0000	0.0000
3	52	-0.0790	20.000	0.21088E-01	0.0000	1.0000	2569.0	0.000	0.000	0.0000	0.0000
3	53	-0.0741	20.000	0.21088E-01	0.0000	1.0000	2569.0	0.000	0.000	0.0000	0.0000
3	54	-0.0692	20.000	0.21088E-01	0.0000	1.0000	2569.0	0.000	0.000	0.0000	0.0000
3	55	-0.0642	20.000	0.21088E-01	0.0000	1.0000	2569.0	0.000	0.000	0.0000	0.0000

REGION	MESH POINT	Z(M)	P(MPA)	RHO(GM/CC)	U(M/S)	EPS(-)	T(DEG.K)	SIGEQ(MPA)	CAV.RAD(CM)	JET MASS(GM/CM)	JET VEL(M/S)
3	56	-0.0593	20.000	0.21088E-01	0.0000	1.0000	2569.0	0.000	0.000	0.0000	0.0000
3	57	-0.0543	20.000	0.21088E-01	0.0000	1.0000	2569.0	0.000	0.000	0.0000	0.0000
3	58	-0.0494	20.000	0.21088E-01	0.0000	1.0000	2569.0	0.000	0.000	0.0000	0.0000
3	59	-0.0445	20.000	0.21088E-01	0.0000	1.0000	2569.0	0.000	0.000	0.0000	0.0000
3	60	-0.0395	20.000	0.21088E-01	0.0000	1.0000	2569.0	0.000	0.000	0.0000	0.0000
3	61	-0.0346	20.000	0.21088E-01	0.0000	1.0000	2569.0	0.000	0.000	0.0000	0.0000
3	62	-0.0296	20.000	0.21088E-01	0.0000	1.0000	2569.0	0.000	0.000	0.0000	0.0000
3	63	-0.0247	20.000	0.21088E-01	0.0000	1.0000	2569.0	0.000	0.000	0.0000	0.0000
3	64	-0.0198	20.000	0.21088E-01	0.0000	1.0000	2569.0	0.000	0.000	0.0000	0.0000
3	65	-0.0148	20.000	0.21088E-01	0.0000	1.0000	2569.0	0.000	0.000	0.0000	0.0000
3	66	-0.0099	20.000	0.21088E-01	0.0000	1.0000	2569.0	0.000	0.000	0.0000	0.0000
3	67	-0.0049	20.000	0.21088E-01	0.0000	1.0000	2569.0	0.000	0.000	0.0000	0.0000
3	68	0.0000	20.000	0.21088E-01	0.0000	1.0000	2569.0	0.000	0.000	0.0000	0.0000
4	69	0.0000	20.000	0.21088E-01	0.0000	1.0000	2569.0	0.000	0.000	0.0000	0.0000
4	70	0.0000	20.000	0.21088E-01	0.0000	1.0000	2569.0	0.000	0.000	0.0000	0.0000

STATE OF COMPOUND PISTON

PISTON	DISP(M)	VEL(M/S)	P.DAMP(MPA)	P.RCVR(MPA)
FORWARD	0.0000	0.000	0.0	0.0
CENTER	0.0000	0.000	0.0	0.0
REAR	0.0000	0.000	0.0	0.0

STEP NUMBER = 8729   TIME(MSEC) = 3.000   DELTA T(MSEC) = 0.0003

PROJECTILE TRAVEL (M)	0.0351
PROJECTILE VELOCITY (M/S)	34.7608
PISTON TRAVEL (CM)	1.1893
PISTON VELOCITY (M/S)	11.8236
UNATOMIZED FRACTION OF BOOSTER CHARGE (%)	89.459
UNATOMIZED FRACTION OF TRAVELING CHARGE (%)	0.000
FRACTION OF TOTAL FUEL IN DROPLET PHASE (%)	0.000
TOTAL MASS (GM)	7614.559

MASS DEFECT (%)	0.091
TOTAL ENERGY (J)	30748540.991
ENERGY DEFECT (%)	0.119
OBTURATOR RESISTANCE (MPA)	10.000
AIR SHOCK RESISTANCE (MPA)	0.115
MASS OF AXIAL JET(GM)	195.650
LENGTH OF AXIAL JET (CM)	2.1661
MAX. LENGTH OF AXIAL JET (CM)	2.1786
RATE OF INJECTION OF JET(GM/S)	951692.
RATE OF DISINTEGRATION OF JET(GM/S)	509418.
TAYLOR JET PARAMETER(-)	0.242957E-29

REGION	MESH POINT	Z(M)	P(MPA)	RHO(GM/CC)	U(M/S)	EPS(-)	T(DEG.K)	SIGEQ(MPA)	CAV.RAD(CM)	JET MASS(GM/CM)	JET VEL(M/S)
1	1	-0.2591	81.731	1.4506	0.0000	0.0000	0.0	0.000	0.000	0.0000	0.0000
1	2	-0.2563	81.737	1.4506	-0.0002	0.0000	0.0	0.000	0.000	0.0000	0.0000
1	3	-0.2535	81.766	1.4506	-0.0006	0.0000	0.0	0.000	0.000	0.0000	0.0000
1	4	-0.2508	81.802	1.4506	0.0038	0.0000	0.0	0.000	0.000	0.0000	0.0000
1	5	-0.2480	81.847	1.4506	0.0121	0.0000	0.0	0.000	0.000	0.0000	0.0000
1	6	-0.2452	81.902	1.4506	0.0247	0.0000	0.0	0.000	0.000	0.0000	0.0000
1	7	-0.2424	81.975	1.4506	0.0401	0.0000	0.0	0.000	0.000	0.0000	0.0000
1	8	-0.2396	82.066	1.4507	0.0584	0.0000	0.0	0.000	0.000	0.0000	0.0000
1	9	-0.2368	82.165	1.4507	0.0798	0.0000	0.0	0.000	0.000	0.0000	0.0000
1	10	-0.2340	82.261	1.4507	0.1036	0.0000	0.0	0.000	0.000	0.0000	0.0000
1	11	-0.2313	82.348	1.4507	0.1280	0.0000	0.0	0.000	0.000	0.0000	0.0000
1	12	-0.2285	82.430	1.4507	0.1515	0.0000	0.0	0.000	0.000	0.0000	0.0000
1	13	-0.2257	82.514	1.4508	0.1748	0.0000	0.0	0.000	0.000	0.0000	0.0000
1	14	-0.2229	82.607	1.4508	0.2021	0.0000	0.0	0.000	0.000	0.0000	0.0000
1	15	-0.2201	82.705	1.4508	0.2380	0.0000	0.0	0.000	0.000	0.0000	0.0000
1	16	-0.2173	82.806	1.4508	0.2834	0.0000	0.0	0.000	0.000	0.0000	0.0000
1	17	-0.2145	82.907	1.4509	0.3342	0.0000	0.0	0.000	0.000	0.0000	0.0000
1	18	-0.2118	83.007	1.4509	0.3842	0.0000	0.0	0.000	0.000	0.0000	0.0000
1	19	-0.2090	83.097	1.4509	0.4310	0.0000	0.0	0.000	0.000	0.0000	0.0000
1	20	-0.2062	83.170	1.4509	0.4760	0.0000	0.0	0.000	0.000	0.0000	0.0000
1	21	-0.2034	83.226	1.4509	0.5214	0.0000	0.0	0.000	0.000	0.0000	0.0000
1	22	-0.2006	83.284	1.4509	0.5664	0.0000	0.0	0.000	0.000	0.0000	0.0000
1	23	-0.1978	83.361	1.4510	0.6091	0.0000	0.0	0.000	0.000	0.0000	0.0000
1	24	-0.1950	83.453	1.4510	0.6512	0.0000	0.0	0.000	0.000	0.0000	0.0000
1	25	-0.1923	83.543	1.4510	0.6963	0.0000	0.0	0.000	0.000	0.0000	0.0000
1	26	-0.1895	83.619	1.4510	0.7429	0.0000	0.0	0.000	0.000	0.0000	0.0000
1	27	-0.1867	83.695	1.4510	0.7830	0.0000	0.0	0.000	0.000	0.0000	0.0000
1	28	-0.1839	83.781	1.4511	0.8121	0.0000	0.0	0.000	0.000	0.0000	0.0000
1	29	-0.1811	83.857	1.4511	0.8367	0.0000	0.0	0.000	0.000	0.0000	0.0000

REGION	MESH POINT	Z(M)	P(MPA)	RHO(GM/CC)	U(M/S)	EPS(-)	T(DEG.K)	SIGEQ(MPA)	CAV.RAD(CM)	JET MASS(GM/CM)	JET VEL(M/S)
1	30	-0.1783	83.904	1.4511	0.8679	0.0000	0.0	0.000	0.000	0.0000	0.0000
1	31	-0.1755	83.932	1.4511	0.9032	0.0000	0.0	0.000	0.000	0.0000	0.0000
1	32	-0.1728	84.016	1.4511	0.9225	0.0000	0.0	0.000	0.000	0.0000	0.0000
1	33	-0.1700	84.193	1.4512	0.9081	0.0000	0.0	0.000	0.000	0.0000	0.0000
3	36	-0.1700	72.142	0.82916E-01	-11.8236	1.0000	2256.7	0.000	0.000	82.15	0.0000
3	37	-0.1647	72.306	0.84355E-01	-10.8914	1.0000	2221.0	0.000	0.000	80.39	0.0000
3	38	-0.1593	72.623	0.87004E-01	-9.4658	1.0000	2158.7	0.000	0.000	67.89	0.0000
3	39	-0.1540	73.071	0.89170E-01	-6.4253	1.0000	2116.0	0.000	0.000	47.25	0.0000
3	40	-0.1487	73.288	0.90730E-01	-10.2213	1.0000	2083.4	0.000	0.000	37.01	116.7
3	41	-0.1434	74.082	0.92007E-01	-4.9516	1.0000	2074.8	0.000	0.000	41.51	112.9
3	42	-0.1381	75.030	0.92772E-01	21.2011	1.0000	2082.9	0.000	0.000	37.29	110.5
3	43	-0.1328	75.011	0.91828E-01	42.6771	1.0000	2105.2	0.000	0.000	14.39	108.0
3	44	-0.1275	74.710	0.89851E-01	43.3500	1.0000	2146.0	0.000	0.000	0.0000	0.0000
3	45	-0.1222	74.582	0.88004E-01	46.7685	1.0000	2190.1	0.000	0.000	0.0000	0.0000
3	46	-0.1169	74.083	0.85888E-01	54.6443	1.0000	2232.5	0.000	0.000	0.0000	0.0000
3	47	-0.1115	73.715	0.83928E-01	59.5404	1.0000	2276.5	0.000	0.000	0.0000	0.0000
3	48	-0.1062	73.340	0.82006E-01	64.0004	1.0000	2321.2	0.000	0.000	0.0000	0.0000
3	49	-0.1009	73.219	0.80311E-01	68.0360	1.0000	2369.2	0.000	0.000	0.0000	0.0000
3	50	-0.0956	73.300	0.78761E-01	73.8122	1.0000	2421.1	0.000	0.000	0.0000	0.0000
3	51	-0.0903	73.486	0.7724[illegible]E-01	81.6643	1.0000	2477.7	0.000	0.000	0.0000	0.0000
3	52	-0.0850	73.630	0.75628E-01	91.0424	1.0000	2538.5	0.000	0.000	0.0000	0.0000
3	53	-0.0797	73.728	0.73933E-01	100.0949	1.0000	2603.2	0.000	0.000	0.0000	0.0000
3	54	-0.0744	73.763	0.72180E-01	108.2523	1.0000	2671.1	0.000	0.000	0.0000	0.0000
3	55	-0.0690	73.804	0.70457E-01	115.0888	1.0000	2741.2	0.000	0.000	0.0000	0.0000
3	56	-0.0637	73.846	0.68804E-01	121.4418	1.0000	2812.0	0.000	0.000	0.0000	0.0000
3	57	-0.0584	73.920	0.67278E-01	127.5319	1.0000	2881.8	0.000	0.000	0.0000	0.0000
3	58	-0.0531	74.015	0.65904E-01	133.5105	1.0000	2948.5	0.000	0.000	0.0000	0.0000
3	59	-0.0478	74.117	0.64698E-01	139.0456	1.0000	3010.2	0.000	0.000	0.0000	0.0000
3	60	-0.0425	74.187	0.63652E-01	143.6017	1.0000	3064.8	0.000	0.000	0.0000	0.0000
3	61	-0.0372	74.192	0.62755E-01	146.5452	1.0000	3110.8	0.000	0.000	0.0000	0.0000
3	62	-0.0319	74.127	0.62000E-01	147.2157	1.0000	3147.6	0.000	0.000	0.0000	0.0000
3	63	-0.0266	73.995	0.61369E-01	144.9945	1.0000	3175.7	0.000	0.000	0.0000	0.0000
3	64	-0.0212	73.871	0.60886E-01	140.3919	1.0000	3196.6	0.000	0.000	0.0000	0.0000
3	65	-0.0159	73.782	0.60539E-01	133.7552	1.0000	3211.9	0.000	0.000	0.0000	0.0000
3	66	-0.0106	73.811	0.60356E-01	126.5066	1.0000	3223.4	0.000	0.000	0.0000	0.0000
3	67	-0.0053	73.984	0.60325E-01	119.2505	1.0000	3232.6	0.000	0.000	0.0000	0.0000
3	68	0.0000	74.317	0.60432E-01	112.5423	1.0000	3241.2	0.000	0.000	0.0000	0.0000
4	69	0.0000	74.317	0.60432E-01	112.5176	1.0000	3241.2	0.000	0.000	0.0000	0.0000
4	70	0.0018	74.453	0.60493E-01	106.9237	1.0000	324[illegible]	0.000	0.000	0.0000	0.0000
4	71	0.0035	74.587	0.60547E-01	101.4520	1.0000	3246.5	0.000	0.000	0.0000	0.0000
4	72	0.0053	74.713	0.60603E-01	96.1331	1.0000	3248.9	0.000	0.000	0.0000	0.0000
4	73	0.0070	74.828	0.60658E-01	90.9840	1.0000	3250.8	0.000	0.000	0.0000	0.0000
4	74	0.0088	74.929	0.60710E-01	86.0324	1.0000	3252.3	0.000	0.000	0.0000	0.0000
4	75	0.0105	75.012	0.60753E-01	81.2931	1.0000	3253.4	0.000	0.000	0.0000	0.0000
4	76	0.0123	75.076	0.60785E-01	76.7781	1.0000	3254.4	0.000	0.000	0.0000	0.0000
4	77	0.0140	75.120	0.60804E-01	72.4911	1.0000	3255.3	0.000	0.000	0.0000	0.0000
4	78	0.0158	75.144	0.60811E-01	68.4305	1.0000	3255.9	0.000	0.000	0.0000	0.0000

REGION	MESH POINT	Z(M)	P(MPA)	RHO(GM/CC)	U(M/S)	EPS(-)	T(DEG.K)	SIGEQ(MPA)	CAV.RAD(CM)	JET MASS(GM/CM)	JET VEL(M/S)
4	79	0.0176	75.149	0.60807E-01	64.5886	1.0000	3256.4	0.000	0.000	0.0000	0.0000
4	80	0.0193	75.137	0.60794E-01	60.9549	1.0000	3256.6	0.000	0.000	0.0000	0.0000
4	81	0.0211	75.112	0.60773E-01	57.5105	1.0000	3256.7	0.000	0.000	0.0000	0.0000
4	82	0.0228	75.077	0.60747E-01	54.2508	1.0000	3256.6	0.000	0.000	0.0000	0.0000
4	83	0.0246	75.036	0.60717E-01	51.1453	1.0000	3256.5	0.000	0.000	0.0000	0.0000
4	84	0.0263	74.993	0.60685E-01	48.1833	1.0000	3256.4	0.000	0.000	0.0000	0.0000
4	85	0.0281	74.951	0.60653E-01	45.3379	1.0000	3256.4	0.000	0.000	0.0000	0.0000
4	86	0.0299	74.914	0.60620E-01	42.5936	1.0000	3256.6	0.000	0.000	0.0000	0.0000
4	87	0.0316	74.385	0.60588E-01	39.9296	1.0000	3257.1	0.000	0.000	0.0000	0.0000
4	88	0.0334	74.864	0.60552E-01	37.2968	1.0000	3258.2	0.000	0.000	0.0000	0.0000
4	89	0.0351	74.858	0.60514E-01	34.7608	1.0000	3260.1	0.000	0.000	0.0000	0.0000

STEP NUMBER =18391   TIME(MSEC) =   6.000   DELTA T(MSEC) =   0.0003

PROJECTILE TRAVEL (M)	0.4502
PROJECTILE VELOCITY (M/S)	289.5238
PISTON TRAVEL (CM)	9.6712
PISTON VELOCITY (M/S)	40.2353
UNATOMIZED FRACTION OF BOOSTER CHARGE (%)	4.539
UNATOMIZED FRACTION OF TRAVELING CHARGE (%)	0.000
FRACTION OF TOTAL FUEL IN DROPLET PHASE (%)	0.000
TOTAL MASS (GM)	7460.562
MASS DEFECT (%)	2.111
TOTAL ENERGY (J)	30206648.848
ENERGY DEFECT (%)	1.879
OBTURATOR RESISTANCE (MPA)	3.000
AIR SHOCK RESISTANCE (MPA)	0.288
MASS OF AXIAL JET(GM)	324.641
LENGTH OF AXIAL JET (CM)	0.9138
MAX. LENGTH OF AXIAL JET (CM)	2.2580
RATE OF INJECTION OF JET(GM/S)	0.318771E+07
RATE OF DISINTEGRATION OF JET(GM/S)	0.000000
TAYLOR JET PAPAMETER(-)	0.669700E-31

REGION	MESH POINT	Z(M)	P(MPA)	RHO(GM/CC)	U(M/S)	EPS(-)	T(DEG.K)	SIGEQ(MPA)	CAV.RAD(CM)	JET MASS(GM/CM)	JET VEL(M/S)
1	1	-0.2591	413.073	1.5161	0.0000	0.0000	0.0	0.000	0.000	0.0000	0.0000
1	2	-0.2570	412.993	1.5161	0.2678	0.0000	0.0	0.000	0.000	0.0000	0.0000
1	3	-0.2548	412.733	1.5160	0.5851	0.0000	0.0	0.000	0.000	0.0000	0.0000
3	6	-0.2548	283.295	0.30244	-40.2353	1.0000	2047.0	0.000	0.000	67.13	0.0000
3	7	-0.2468	282.345	0.30274	-25.4555	1.0000	2037.6	0.000	0.000	67.74	0.0000
3	8	-0.2389	284.110	0.30422	-5.6499	1.0000	2037.8	0.000	0.000	67.87	0.0000
3	9	-0.2309	288.011	0.30602	17.6775	1.0000	2050.5	0.000	0.000	67.64	0.0000
3	10	-0.2229	287.199	0.30477	23.3593	1.0000	2055.3	0.000	0.000	69.33	0.0000
3	11	-0.2150	288.106	0.30459	27.4324	1.0000	2063.3	0.000	0.000	59.05	0.0000
3	12	-0.2070	291.295	0.30564	48.7272	1.0000	2077.1	0.000	0.000	29.59	0.0000
3	13	-0.1991	288.267	0.30236	56.9269	1.0000	2083.6	0.000	0.000	0.0000	0.0000
3	14	-0.1911	288.214	0.30141	53.1735	1.0000	2091.5	0.000	0.000	0.0000	0.0000
3	15	-0.1831	287.917	0.30074	55.3780	1.0000	2095.2	0.000	0.000	0.0000	0.0000
3	16	-0.1752	290.163	0.30207	62.9631	1.0000	2099.9	0.000	0.000	0.0000	0.0000
3	17	-0.1672	295.029	0.30523	74.6169	1.0000	2107.3	0.000	0.000	0.0000	0.0000
3	18	-0.1592	301.193	0.30969	86.7720	1.0000	2112.3	0.000	0.000	0.0000	0.0000
3	19	-0.1513	306.964	0.31438	90.1880	1.0000	2112.1	0.000	0.000	0.0000	0.0000
3	20	-0.1433	311.939	0.31821	93.4349	1.0000	2113.5	0.000	0.000	0.0000	0.0000
3	21	-0.1354	315.481	0.32004	96.7708	1.0000	2122.0	0.000	0.000	0.0000	0.0000
3	22	-0.1274	319.363	0.32126	105.4264	1.0000	2137.6	0.000	0.000	0.0000	0.0000
3	23	-0.1194	322.137	0.32166	117.2860	1.0000	2152.8	0.000	0.000	0.0000	0.0000
3	24	-0.1115	325.570	0.32273	127.5721	1.0000	2166.5	0.000	0.000	0.0000	0.0000
3	25	-0.1035	327.823	0.32341	138.1381	1.0000	2175.6	0.000	0.000	0.0000	0.0000
3	26	-0.0955	329.471	0.32396	144.8253	1.0000	2181.8	0.000	0.000	0.0000	0.0000
3	27	-0.0876	329.346	0.32351	149.9582	1.0000	2184.8	0.000	0.000	0.0000	0.0000
3	28	-0.0796	329.146	0.32303	154.7180	1.0000	2187.7	0.000	0.000	0.0000	0.0000
3	29	-0.0717	329.924	0.32311	164.5474	1.0000	2192.2	0.000	0.000	0.0000	0.0000
3	30	-0.0637	332.782	0.32441	182.1474	1.0000	2199.9	0.000	0.000	0.0000	0.0000
3	31	-0.0557	337.397	0.32670	208.3995	1.0000	2210.3	0.000	0.000	0.0000	0.0000
3	32	-0.0478	342.672	0.32930	241.4433	1.0000	2222.1	0.000	0.000	0.0000	0.0000
3	33	-0.0398	347.017	0.33125	278.4155	1.0000	2233.2	0.000	0.000	0.0000	0.0000
3	34	-0.0318	349.843	0.33224	318.6831	1.0000	2242.8	0.000	0.000	0.0000	0.0000
3	35	-0.0239	350.209	0.33173	361.0105	1.0000	2249.6	0.000	0.000	0.0000	0.0000
3	36	-0.0159	348.666	0.33009	408.7704	1.0000	2254.0	0.000	0.000	0.0000	0.0000
3	37	-0.0080	343.776	0.32646	462.0661	1.0000	2254.2	0.000	0.000	0.0000	0.0000
3	38	0.0000	335.136	0.32056	525.3973	1.0000	2249.5	0.000	0.000	0.0000	0.0000
4	39	0.0000	335.135	0.32056	525.3734	1.0000	2249.5	0.000	0.000	0.0000	0.0000
4	40	0.0225	331.398	0.31640	485.9399	1.0000	2261.7	0.000	0.000	0.0000	0.0000
4	41	0.0450	336.611	0.31744	441.6734	1.0000	2287.8	0.000	0.000	0.0000	0.0000
4	42	0.0675	328.115	0.30980	367.5784	1.0000	2300.0	0.000	0.000	0.0000	0.0000
4	43	0.0900	295.560	0.28662	274.9250	1.0000	2283.9	0.000	0.000	0.0000	0.0000
4	44	0.1126	259.531	0.26070	224.6724	1.0000	2259.2	0.000	0.000	0.0000	0.0000
4	45	0.1351	235.772	0.24106	223.9371	1.0000	2249.2	0.000	0.000	0.0000	0.0000
4	46	0.1576	223.891	0.23006	245.5675	1.0000	2257.8	0.000	0.000	0.0000	0.0000
4	47	0.1801	220.518	0.22504	271.1909	1.0000	2282.6	0.000	0.000	0.0000	0.0000

REGION	MESH POINT	Z(M)	P(MPA)	RHO(GM/CC)	U(M/S)	EPS(-)	T(DEG.K)	SIGEQ(MPA)	CAV.RAD(CM)	JET MASS(GM/CM)	JET VEL(M/S)
4	48	0.2026	222.407	0.22363	297.4882	1.0000	2319.3	0.000	0.000	0.0000	0.0000
4	49	0.2251	227.443	0.22413	324.6652	1.0000	2365.5	0.000	0.000	0.0000	0.0000
4	50	0.2476	234.270	0.22533	351.6731	1.0000	2421.2	0.000	0.000	0.0000	0.0000
4	51	0.2701	243.469	0.22729	374.1085	1.0000	2490.7	0.000	0.000	0.0000	0.0000
4	52	0.2927	256.793	0.23066	385.6523	1.0000	2581.6	0.000	0.000	0.0000	0.0000
4	53	0.3152	273.554	0.23426	382.8450	1.0000	2700.1	0.000	0.000	0.0000	0.0000
4	54	0.3377	292.424	0.23650	387.4441	1.0000	2853.9	0.000	0.000	0.0000	0.0000
4	55	0.3602	306.394	0.23313	410.2991	1.0000	3041.6	0.000	0.000	0.0000	0.0000
4	56	0.3827	316.140	0.22515	451.4960	1.0000	3270.5	0.000	0.000	0.0000	0.0000
4	57	0.4052	330.960	0.21744	485.0271	1.0000	3566.9	0.000	0.000	0.0000	0.0000
4	58	0.4277	339.312	0.20550	421.5361	1.0000	3906.0	0.000	0.000	0.0000	0.0000
4	59	0.4502	343.439	0.19316	289.5238	1.0000	4247.0	0.000	0.000	0.0000	0.0000

STEP NUMBER =22227   TIME(MSEC) =   15.000   DELTA T(MSEC) =   0.0018

PROJECTILE TRAVEL (M)	5.5734
PROJECTILE VELOCITY (M/S)	690.7966
PISTON TRAVEL (CM)	10.1040
PISTON VELOCITY (M/S)	0.0000
UNATOMIZED FRACTION OF BOOSTER CHARGE (%)	0.000
UNATOMIZED FRACTION OF TRAVELING CHARGE (%)	0.000
FRACTION OF TOTAL FUEL IN DROPLET PHASE (%)	0.000
TOTAL MASS (GM)	7498.957
MASS DEFECT (%)	1.608
TOTAL ENERGY (J)	30295210.044
ENERGY DEFECT (%)	1.591
OBTURATOR RESISTANCE (MPA)	3.000
AIR SHOCK RESISTANCE (MPA)	0.863
MASS OF AXIAL JET(GM)	0.000
LENGTH OF AXIAL JET (CM)	**********
MAX. LENGTH OF AXIAL JET (CM)	2.2580
RATE OF INJECTION OF JET(GM/S)	0.000000
RATE OF DISINTEGRATION OF JET(GM/S)	0.000000
TAYLOR JET PARAMETER(-)	0.716509E-31

REGION	MESH POINT	Z(M)	P(MPA)	RHO(GM/CC)	U(M/S)	EPS(-)	T(DEG.K)	SIGEQ(MPA)	CAV.RAD(CM)	JET MASS(GM/CM)	JET VEL(M/S)
REGION	1 IS CLOSED										
3	5	-0.2590	37.486	0.69333E-01	0.0000	1.0000	1416.0	0.000	0.000	0.0000	0.0000
3	6	-0.2509	37.486	0.69395E-01	0.9818	1.0000	1414.7	0.000	0.000	0.0000	0.0000
3	7	-0.2428	37.486	0.69445E-01	1.9632	1.0000	1413.6	0.000	0.000	0.0000	0.0000
3	8	-0.2347	37.486	0.69486E-01	2.9444	1.0000	1412.7	0.000	0.000	0.0000	0.0000
3	9	-0.2266	37.486	0.69517E-01	3.9254	1.0000	1412.1	0.000	0.000	0.0000	0.0000
3	10	-0.2185	37.486	0.69540E-01	4.9064	1.0000	1411.6	0.000	0.000	0.0000	0.0000
3	11	-0.2104	37.486	0.69554E-01	5.8869	1.0000	1411.3	0.000	0.000	0.0000	0.0000
3	12	-0.2023	37.486	0.69561E-01	6.8682	1.0000	1411.2	0.000	0.000	0.0000	0.0000
3	13	-0.1943	37.486	0.69561E-01	7.8478	1.0000	1411.2	0.000	0.000	0.0000	0.0000
3	14	-0.1862	37.486	0.69555E-01	8.8306	1.0000	1411.3	0.000	0.000	0.0000	0.0000
3	15	-0.1781	37.486	0.69543E-01	9.8074	1.0000	1411.5	0.000	0.000	0.0000	0.0000
3	16	-0.1700	37.486	0.69528E-01	10.7953	1.0000	1411.9	0.000	0.000	0.0000	0.0000
3	17	-0.1619	37.486	0.69508E-01	11.7627	1.0000	1412.3	0.000	0.000	0.0000	0.0000
3	18	-0.1538	37.486	0.69484E-01	12.1319	1.0000	1412.8	0.000	0.000	0.0000	0.0000
3	19	-0.1457	37.487	0.69454E-01	12.2575	1.0000	1413.5	0.000	0.000	0.0000	0.0000
3	20	-0.1376	37.489	0.69423E-01	12.7459	1.0000	1414.2	0.000	0.000	0.0000	0.0000
3	21	-0.1295	37.488	0.69391E-01	14.3065	1.0000	1414.9	0.000	0.000	0.0000	0.0000
3	22	-0.1214	37.488	0.69361E-01	16.2834	1.0000	1415.5	0.000	0.000	0.0000	0.0000
3	23	-0.1133	37.486	0.69334E-01	18.4424	1.0000	1416.0	0.000	0.000	0.0000	0.0000
3	24	-0.1052	37.485	0.69311E-01	20.8001	1.0000	1416.4	0.000	0.000	0.0000	0.0000
3	25	-0.0971	37.483	0.69291E-01	23.3885	1.0000	1416.8	0.000	0.000	0.0000	0.0000
3	26	-0.0890	37.480	0.69273E-01	26.2422	1.0000	1417.1	0.000	0.000	0.0000	0.0000
3	27	-0.0809	37.476	0.69258E-01	29.4066	1.0000	1417.3	0.000	0.000	0.0000	0.0000
3	28	-0.0728	37.471	0.69244E-01	32.9320	1.0000	1417.4	0.000	0.000	0.0000	0.0000
3	29	-0.0648	37.465	0.69231E-01	36.8879	1.0000	1417.4	0.000	0.000	0.0000	0.0000
3	30	-0.0567	37.456	0.69217E-01	41.3445	1.0000	1417.4	0.000	0.000	0.0000	0.0000
3	31	-0.0486	37.446	0.69202E-01	46.4223	1.0000	1417.3	0.000	0.000	0.0000	0.0000
3	32	-0.0405	37.430	0.69182E-01	52.2022	1.0000	1417.1	0.000	0.000	0.0000	0.0000
3	33	-0.0324	37.413	0.69162E-01	58.9412	1.0000	1416.9	0.000	0.000	0.0000	0.0000
3	34	-0.0243	37.381	0.69123E-01	66.6323	1.0000	1416.5	0.000	0.000	0.0000	0.0000
3	35	-0.0162	37.358	0.69098E-01	76.0276	1.0000	1416.2	0.000	0.000	0.0000	0.0000
3	36	-0.0081	37.279	0.68995E-01	86.3966	1.0000	1415.5	0.000	0.000	0.0000	0.0000
3	37	0.0000	37.255	0.68971E-01	100.2946	1.0000	1415.0	0.000	0.000	0.0000	0.0000
4	38	0.0000	37.255	0.68971E-01	100.3003	1.0000	1415.0	0.000	0.000	0.0000	0.0000
4	39	0.2787	37.277	0.69447E-01	133.4011	1.0000	1405.7	0.000	0.000	0.0000	0.0000
4	40	0.5573	37.188	0.69695E-01	167.8393	1.0000	1397.1	0.000	0.000	0.0000	0.0000
4	41	0.8360	36.672	0.69203E-01	204.4075	1.0000	1388.0	0.000	0.000	0.0000	0.0000
4	42	1.1147	36.052	0.68451E-01	234.2719	1.0000	1380.3	0.000	0.000	0.0000	0.0000
4	43	1.3933	35.369	0.67532E-01	256.4420	1.0000	1373.4	0.000	0.000	0.0000	0.0000
4	44	1.6720	34.545	0.66356E-01	278.4655	1.0000	1366.4	0.000	0.000	0.0000	0.0000
4	45	1.9507	33.943	0.65467E-01	299.8693	1.0000	1361.6	0.000	0.000	0.0000	0.0000
4	46	2.2293	33.480	0.64740E-01	326.6272	1.0000	1358.8	0.000	0.000	0.0000	0.0000
4	47	2.5080	33.284	0.64352E-01	355.7196	1.0000	1359.4	0.000	0.000	0.0000	0.0000
4	48	2.7867	33.327	0.64226E-01	386.0692	1.0000	1364.0	0.000	0.000	0.0000	0.0000
4	49	3.0654	33.407	0.63999E-01	418.6676	1.0000	1372.3	0.000	0.000	0.0000	0.0000
4	50	3.3440	33.397	0.63405E-01	451.7626	1.0000	1385.3	0.000	0.000	0.0000	0.0000
4	51	3.6227	33.195	0.62223E-01	484.6950	1.0000	1404.3	0.000	0.000	0.0000	0.0000
4	52	3.9014	32.873	0.60479E-01	514.3296	1.0000	1432.5	0.000	0.000	0.0000	0.0000

REGION	MESH POINT	Z(M)	P(MPA)	RHO(GM/CC)	U(M/S)	EPS(-)	T(DEG.K)	SIGEQ(MPA)	CAV.RAD(CM)	JET MASS(GM/CM)	JET VEL(M/S)
4	53	4.1800	32.485	0.58144E-01	541.8584	1.0000	1474.9	0.000	0.000	0.0000	0.0000
4	54	4.4587	31.927	0.54896E-01	570.5611	1.0000	1538.8	0.000	0.000	0.0000	0.0000
4	55	4.7374	31.374	0.50831E-01	600.9801	1.0000	1637.8	0.000	0.000	0.0000	0.0000
4	56	5.0160	31.020	0.46036E-01	631.1365	1.0000	1793.9	0.000	0 000	0.0000	0.0000
4	57	5.2947	30.797	0.40521E-01	659.9999	1.0000	2031.3	0.000	0.000	0.0000	0.0000
4	58	5.5734	30.647	0.34376E-01	690.7966	1.0000	2393.0	0.000	0.000	0.0000	0.0000

SUMMARY OUTPUT

				MIN	MAX
MUZZLE VELOCITY	(M/S)	696.	MASS ERROR (%)	0.000	2.438
MAX. PISTON VELOCITY	(M/S)	40.	ENERGY ERROR (%)	0.000	2.496
MAX. LIQUID PRESSURE	(MPA)	502.29			
MAX. INT. CHAMBER PRESSURE	(MPA)	0.00	THERMO. EFF. (%)	34.024	
MAX. CHAMBER PRESSURE	(MPA)	400.47	PIEZO. EFF. (%)	23.42	
MAX. BARREL PRESSURE	(MPA)	423.44			
MAX. ACCELERATION	(K-G)	19.			

MAX. LIQUID PRESSURE

TIME	TRAVEL	VELOCITY	ACCEL	---------PRESSURE	(MPA)----------			Z	NSTEP
MS	M	M/S	KG	LIQUID	CHAMBER	THROAT	BASE		
5.60	0.345	246.42	9.47	502.29	382.18	268.77	215.84	0.7898	16906

MAX. INTER. CHAMBER PRESSURE

TIME	TRAVEL	VELOCITY	ACCEL	---------PRESSURE	(MPA)----------			Z	NSTEP
MS	M	M/S	KG	LIQUID	CHAMBER	THROAT	BASE		
0.00	0.000	0.00	0.00	0.00	0.00	0.00	0.00	0.0000	0

MAX. CHAMBER PRESSURE

TIME	TRAVEL	VELOCITY	ACCEL	---------PRESSURE	(MPA)----------			Z	NSTEP
MS	M	M/S	KG	LIQUID	CHAMBER	THROAT	BASE		
5.75	0.381	262.81	10.73	369.51	252.48	398.97	243.93	0.8518	17452

MAX. BARREL PRESSURE

TIME	TRAVEL	VELOCITY	ACCEL	---------PRESSURE (MPA)----------				Z	NSTEP
MS	M	M/S	KG	LIQUID	CHAMBER	THROAT	BASE		
5.18	0.251	192.42	18.72	342.77	249.70	221.47	423.44	0.6322	15359

MAX. ACCELERATION

TIME	TRAVEL	VELOCITY	ACCEL	---------PRESSURE (MPA)----------				Z	NSTEP
MS	M	M/S	KG	LIQUID	CHAMBER	THROAT	BASE		
5.18	0.251	192.42	18.72	342.77	249.70	221.48	423.42	0.6322	15360

MAX. PISTON VELOCITY

TIME	TRAVEL	VELOCITY	ACCEL	---------PRESSURE (MPA)----------				Z	NSTEP
MS	M	M/S	KG	LIQUID	CHAMBER	THROAT	BASE		
5.99	0.447	287.71	13.66	428.07	297.32	321.86	310.77	0.9491	18348

BURNOUT OF BOOSTER

TIME	TRAVEL	VELOCITY	ACCEL	---------PRESSURE (MPA)----------				Z	NSTEP
MS	M	M/S	KG	LIQUID	CHAMBER	THROAT	BASE		
6.11	0.482	305.36	12.83	396.92	273.30	298.68	291.14	0.9990	18513

MAX. DROPLET FRACTION

TIME	TRAVEL	VELOCITY	ACCEL	---------PRESSURE (MPA)----------				Z	NSTEP
MS	M	M/S	KG	LIQUID	CHAMBER	THROAT	BASE		
15.50	5.918	696.37	1.10	0.00	34.77	34.54	28.50	1.0000	22401

MUZZLE

TIME	TRAVEL	VELOCITY	ACCEL	---------PRESSURE (MPA)----------				Z	NSTEP
MS	M	M/S	KG	LIQUID	CHAMBER	THROAT	BASE		
15.50	5.918	696.37	1.10	0.00	34.77	34.54	28.50	1.0000	22401

1 ENERGY BALANCE SUMMARY	KILO-JOULES	PERCENT
TOTAL CHEMICAL:	30280.552	100.00
(1) UNBURNT CHEMICAL:	0.000	0.00
(2) TOTAL GAS INTERNAL ENERGY:	17478.612	57.72
(3) WORK AND LOSSES:	11035.581	36.44
(A) PROJECTILE KINETIC:	10474.418	34.59
(B) PISTON KINETIC:	0.000	0.00
(C) LIQUID KINETIC:	0.000	0.00
(D) GAS KINETIC:	556.233	1.84
(E) HEAT LOSS:	1766.359	5.83
(F) FRICTION AND AIR SHOCK WORK	4.931	0.02

INTENTIONALLY LEFT BLANK.

No. of Copies	Organization
2	Administrator Defense Technical Info Center ATTN: DTIC-DDA Cameron Station Alexandria, VA 22304-6145
1	Commander U.S. Army Materiel Command ATTN: AMCAM 5001 Eisenhower Ave. Alexandria, VA 22333-0001
1	Director U.S. Army Research Laboratory ATTN: AMSRL-D 2800 Powder Mill Rd. Adelphi, MD 20783-1145
1	Director U.S. Army Research Laboratory ATTN: AMSRL-OP-CI-AD, Tech Publishing 2800 Powder Mill Rd. Adelphi, MD 20783-1145
2	Commander U.S. Army Armament Research, Development, and Engineering Center ATTN: SMCAR-IMI-I Picatinny Arsenal, NJ 07806-5000
2	Commander U.S. Army Armament Research, Development, and Engineering Center ATTN: SMCAR-TDC Picatinny Arsenal, NJ 07806-5000
1	Director Benet Weapons Laboratory U.S. Army Armament Research, Development, and Engineering Center ATTN: SMCAR-CCB-TL Watervliet, NY 12189-4050
(Unclass. only) 1	Commander U.S. Army Rock Island Arsenal ATTN: SMCRI-IMC-RT/Technical Library Rock Island, IL 61299-5000
1	Director U.S. Army Aviation Research and Technology Activity ATTN: SAVRT-R (Library) M/S 219-3 Ames Research Center Moffett Field, CA 94035-1000

No. of Copies	Organization
1	Commander U.S. Army Missile Command ATTN: AMSMI-RD-CS-R (DOC) Redstone Arsenal, AL 35898-5010
1	Commander U.S. Army Tank-Automotive Command ATTN: ASQNC-TAC-DIT (Technical Information Center) Warren, MI 48397-5000
1	Director U.S. Army TRADOC Analysis Command ATTN: ATRC-WSR White Sands Missile Range, NM 88002-5502
1	Commandant U.S. Army Field Artillery School ATTN: ATSF-CSI Ft. Sill, OK 73503-5000
(Class. only) 1	Commandant U.S. Army Infantry School ATTN: ATSH-CD (Security Mgr.) Fort Benning, GA 31905-5660
(Unclass. only) 1	Commandant U.S. Army Infantry School ATTN: ATSH-CD-CSO-OR Fort Benning, GA 31905-5660
1	WL/MNOI Eglin AFB, FL 32542-5000
	<u>Aberdeen Proving Ground</u>
2	Dir, USAMSAA ATTN: AMXSY-D AMXSY-MP, H. Cohen
1	Cdr, USATECOM ATTN: AMSTE-TC
1	Dir, ERDEC ATTN: SCBRD-RT
1	Cdr, CBDA ATTN: AMSCB-CI
1	Dir, USARL ATTN: AMSRL-SL-I
10	Dir, USARL ATTN: AMSRL-OP-CI-B (Tech Lib)

No. of Copies	Organization
1	OSD/SDIO/IST ATTN: Dr. Len Caveny Pentagon Washington, DC 20301-7100
1	Commander U.S. Army Armament Research, Development, and Engineering Center ATTN: SMCAR-TSS Picatinny Arsenal, NJ 07806-5000
4	Commander U.S. Army Armament Research, Development, and Engineering Center ATTN: SMCAR-AEE-BR, A. Beardell SMCAR-AEE-B, D. Downs SMCAR-AEE, A. Bracuti D. Chieu Picatinny Arsenal, NJ 07806-5000
1	Commander U.S. Army Armament Research, Development, and Engineering Center ATTN: SMCAR-FSA-S, H. Liberman Picatinny Arsenal, NJ 07806-5000
8	Commander U.S. Army Armament Research, Development, and Engineering Center ATTN: SMCAR-FSS-DA, Bldg 94, B. Machak S. Traendly T. Kuriata R. Kopmann J. Irizarry L. Pinder C. Spinelli K. Chung Picatinny Arsenal, NJ 07806-5000
2	Commandant U.S. Army Field Artillery School ATTN: ATSF-CMW ATSF-TSM-CN, J. Spicer Fort Sill, OK 73503

No. of Copies	Organization
1	Commander U.S. Army Belvoir RD&E Center ATTN: STRBE-WC, Tech Library (Vault) B-315 Fort Belvoir, VA 22060-5606
1	Commander U.S. Army Research Office ATTN: Technical Library P.O. Box 12211 Research Triangle Park, NC 27709-2211
1	Commandant U.S. Army Armor Center ATTN: ATSB-CD-MLD Fort Knox, KY 40121
4	Commander Dahlgren Division Naval Surface Warfare Center ATTN: Code G30, Guns and Munitions Division Code G301, D. Wilson Code G32, Gun Systems Branch Code E23, Technical Library Dahlgren, VA 22448-5000
2	Commander Naval Surface Warfare Center ATTN: O. Dengel K. Thorsted Silver Spring, MD 20902-5000
1	Commander Naval Weapons Center China Lake, CA 93555-6001
1	Director Benet Laboratories U.S. Army Armament Research, Development, and Engineering Center ATTN: SMCAR-CCB-RA, Julius Frankel Watervliet, NY 12189-4050
1	Commandant USAFAS ATTN: ATSF-TSM-CN Fort Sill, OK 73503-5600

No. of Copies	Organization
1	HQ USAMC COM AMSMC-SAS ATTN: George Schlenker Rock Island, IL 61299-6000
1	California Institute of Technology Jet Propulsion Laboratory ATTN: Technical Library 4800 Oak Grove Drive Pasadena, CA 91109
2	Sandia National Laboratories, Livermore Combustion Research Facility Division 8357 ATTN: Dr. S. Vosen Dr. R. Armstrong Livermore, CA 94551-0469
2	Director National Aeronautics and Space Administration Lewis Research Center ATTN: MS-603, Technical Library MS-86, Dr. Povinelli 21000 Brookpark Road Cleveland, OH 44135
1	Director National Aeronautics and Space Administration Manned Spacecraft Center Houston, TX 77058
1	The Johns Hopkins University Applied Physics Laboratory Johns Hopkins Road Laurel, MD 20707
1	University of Illinois at Chicago Department of Chemical Engineering ATTN: Professor Sohail Murad Box 4348 Chicago, IL 60680
1	University of Missouri at Columbia Department of Chemistry ATTN: Professor R. Thompson Columbia, MO 65211

No. of Copies	Organization
1	University of Michigan ATTN: Professor Gerard M. Faeth Department of Aerospace Engineering Ann Arbor, MI 48109-3796
1	University of Missouri at Kansas City Department of Physics ATTN: Professor R. D. Murphy 1110 East 48th Street Kansas City, MO 64110-2499
1	Pennsylvania State University Department of Mechanical Engineering ATTN: Professor K. Kuo University Park, PA 16802
1	University of Arkansas Department of Chemical Engineering ATTN: J. Havens 227 Engineering Building Fayetteville, AR 72701
2	University of Delaware Department of Chemistry ATTN: Mr. James Cronin Professor Thomas Brill Newark, DE 19711
1	Institute of Advanced Technology ATTN: Dr. Harry Fair 4030-2 W. Braker Lane Austin, TX 78759-5329
1	School of Engineering and Computer Science California State Univesity, Sacramento ATTN: Dr. Frederick Reardon 6000 J St. Sacramento, CA 95819-2694
1	University of Colorado at Boulder Department of Mechanical Engineering ATTN: Dr. John Daily Engineering Center ME 1-13 Campus Box 427 Boulder, CO 80309-0427

No. of Copies	Organization
1	University of Maryland at College Park ATTN: Professor Franz Kasler Department of Chemistry College Park, MD 20742
1	Director Sandia National Laboratories Division 8152 ATTN: Dr. Ray Rychnovsky P.O. Box 969 Livermore, CA 94551-0969
1	Director Sandia National Laboratories Division 8244 ATTN: Dr. Stuart Griffiths P.O. Box 969 Livermore, CA 94551-0969
2	Princeton Combustion Research Laboratories, Inc. ATTN: Neale A. Messina Dr. Martin Summerfield Princeton Corporate Plaza 11 Deerpark Dr., Bldg. IV, Suite 119 Monmouth Junction, NJ 08852
1	Conway Enterprises ATTN: Professor Alistair Macpherson 499 Pine Top Trial Bethlehem, PA 18017-1828
1	Paul Gough Associates, Inc. ATTN: Dr. Paul S. Gough 1048 South Street Portsmouth, NH 03801-5423
1	IITRI ATTN: Library 10 W. 35th St Chicago, IL 60616
1	Science Applications International Corporation ATTN: Norman Banks Suite 255 4900 Waters Edge Drive Raleigh, NC 27606

No. of Copies	Organization
1	Calspan Corporation ATTN: Technical Library P.O. Box 400 Buffalo, NY 14225
6	General Electric Ord Sys Div ATTN: J. Mandzy, OP43-220 R. E. Mayer W. Pasko B. Haberl I. Magoon L. A. Walter 100 Plastics Avenue Pittsfield, MA 01201-3698
1	Sundstrand Aviation Operations ATTN: Mr. Owen Briles P.O. Box 7202 Rockford, IL 61125
1	Veritay Technology, Inc. ATTN: E. B. Fisher P.O. Box 305 4845 Millersport Highway East Amherst, NY 14051-0305
2	Science Applications International Corporation ATTN: Dr. Sanford Dash Mr. Neeraj Sinha 501 Office Center Drive Suite 420 Ft. Washington, PA 19034-3211
1	Georgia Institute of Technology School of Aerospace Engineering ATTN: Dr. Suresh Menon Atlanta, GA 30332-0150
2	Institute for Defense Analysis ATTN: Dr. Joan Cartier Dr. David Sparrow 1801 N. Beauregard St. Alexandria, VA 22311-1772

No. of Copies	Organization
1	RARDE GS2 Division ATTN: Dr. Clive Woodley Building R31 Ft. Halstead Sevenoaks, Kent TN14 7BT ENGLAND
1	Imperial College of Science and Medicine Mechanical Engineering Department ATTN: Professor J. H. Whitelaw Exhibition Road, London SW7 2BX ENGLAND

INTENTIONALLY LEFT BLANK.